



Deposited via The University of Sheffield.

White Rose Research Online URL for this paper:

<https://eprints.whiterose.ac.uk/id/eprint/204588/>

Version: Published Version

Article:

Al Sheikh Omar, A., Salehi, F.M., Bai, M. et al. (2023) In situ nanocompression of carbon black to understand the tribology of contaminated diesel engine oils. *Carbon*, 212. 118170. ISSN: 0008-6223

<https://doi.org/10.1016/j.carbon.2023.118170>

Reuse

This article is distributed under the terms of the Creative Commons Attribution (CC BY) licence. This licence allows you to distribute, remix, tweak, and build upon the work, even commercially, as long as you credit the authors for the original work. More information and the full terms of the licence here:

<https://creativecommons.org/licenses/>

Takedown

If you consider content in White Rose Research Online to be in breach of UK law, please notify us by emailing eprints@whiterose.ac.uk including the URL of the record and the reason for the withdrawal request.

Carbon

Probing the Mechanical Properties of Soot to Understand the Tribology of Contaminated Diesel Engine Oils

--Manuscript Draft--

Manuscript Number:	CARBON-D-23-00599
Article Type:	Research Paper
Keywords:	Soot; In situ SEM; Nanoindentation; Crystal structure; Mechanical properties; Tribology
Corresponding Author:	Alaaeddin Al Sheikh Omar, PhD IFS LEEDS, UNITED KINGDOM
First Author:	Alaaeddin Institute of Functional Surfaces Al Sheikh Omar, PhD
Order of Authors:	Alaaeddin Institute of Functional Surfaces Al Sheikh Omar, PhD Farnaz Motamen Salehi, Phd Mingwen Bai, Phd Beverley J. Jnkson, Professor Ardian Morina
Abstract:	<p>The study has evaluated the role of soot in affecting the performance of engine oils. It is very well known that the existence of soot in oil produces abrasive wear on the contact surfaces. Other mechanisms influence the oil performance such as additives adsorption on soot and oil degradation due to the interactions with soot. Recent research has suggested the existence of another wear mechanism related to soot particles, which remains poorly understood. This study investigates the effect of soot interactions in engine oil on its mechanical properties. Carbon black particles (CBPs) were used in the experiments to simulate real soot in the engine. The microstructure and crystal structure of CBPs compared to real soot were investigated using transmission electron microscopy (TEM) and X-ray diffraction (XRD). In situ compression of the single particle was conducted in a scanning electron microscope (SEM) to evaluate the mechanical properties of fresh and aged CBPs with different sizes (100-200 nm). The results show that aged CBPs are significantly harder than fresh CBPs, indicating that ageing in oil modifies the turbostratic crystal structure of soot and alters its mechanical properties, potentially affecting tribological performance.</p>
Suggested Reviewers:	<p>Tom Slatter, PhD, MEng, PGCertEd Professor tom.slatter@sheffield.ac.uk Prof. Tom has been investigating in the area similar to our subject</p> <p>Rob Dwyer-Joyce, Phd Professor, The University of Sheffield Department of Mechanical Engineering r.dwyer-joyce@sheffield.ac.uk Prof.Rob has been studied and supervised many subjects related to our study.</p> <p>Liuquan Yang, Phd Lecturer l.q.yang@leeds.ac.uk Dr Liu has been studying the Graphene and carbon materials.</p>
Opposed Reviewers:	

Declaration of interests

The authors declare that they have no known competing financial interests or personal relationships that could have appeared to influence the work reported in this paper.

The authors declare the following financial interests/personal relationships which may be considered as potential competing interests:

01 March 2023

Dear Dr. Terrones and Dr Neighbour

We wish to submit a new manuscript entitled “Probing the Mechanical Properties of Soot to Understand the Tribology of Contaminated Diesel Engine Oils ” for consideration by Carbon Journal.

We confirm that this work is original and has not been published elsewhere, nor is it currently under consideration for publication elsewhere.

In this paper, the work aims to This study investigates the effect of soot interactions in engine oil on its mechanical properties. Carbon black particles (CBPs) were used in the experiments to simulate real soot in the engine. The results of this study will help to understand whether the change in mechanical properties of soot particles is due to chemical interactions with oil/additives occurs, which potentially affects tribological performance. Carbon Journal has been considered by many researchers to publish and read topics related to carbon materials. Therefore, we are honoured to select the Carbon journal to present our work.

Thank you for your consideration of this manuscript.

Sincerely,

Dr. Aladdin

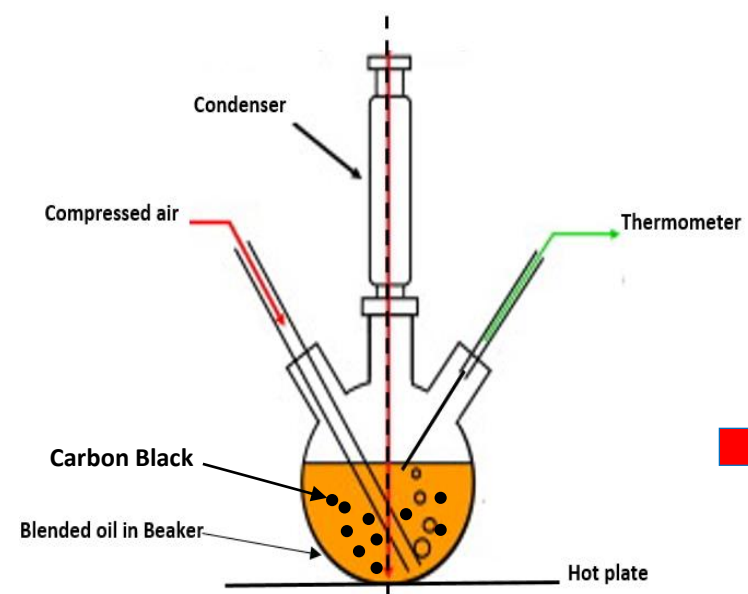
University of Leeds, UK

Checklist for New Submissions

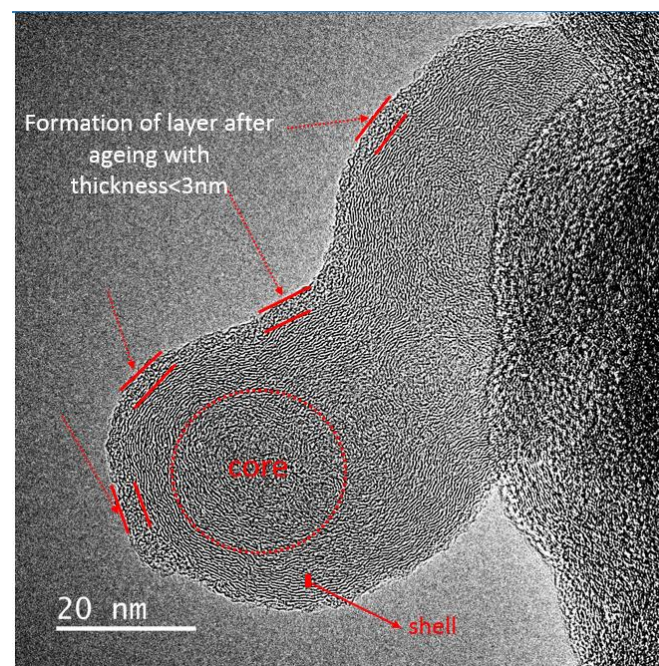
Manuscript	
Figures	
Cover letter	
Graphical abstract	
Declaration of Interest Statement	
Credit author statement	

Credit Author Statement

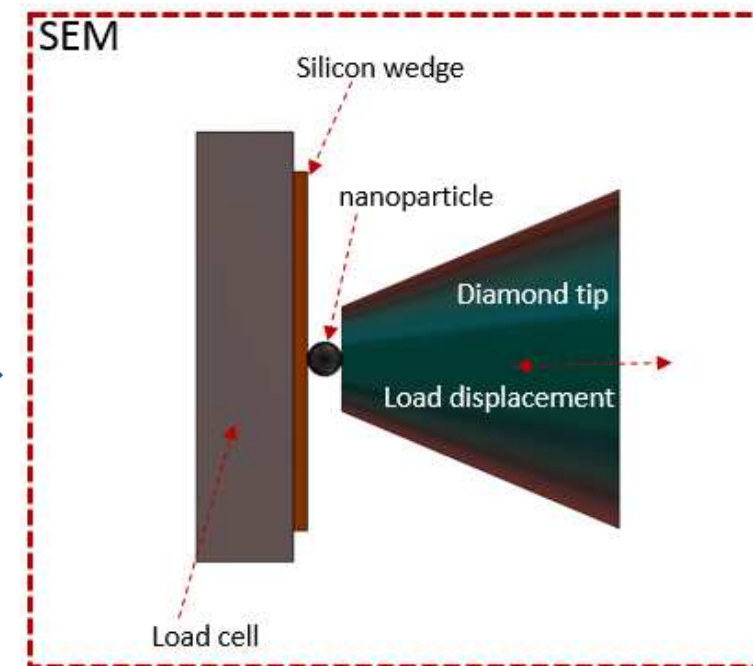
A. Al Sheikh Omar carried out the Lab experiments and wrote the draft manuscript. M. Bai conducted SEM Nanocompression tests, A. Al Sheikh Omar, F. Motamen Salehi, M. Bai, B. J. Jnkson, A. Morina, contributed in reviewing and editing of the manuscript.



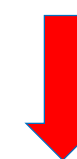
1 Ageing carbon black



2 Changes in carbon black microstructure after ageing



3 SEM nanoindentation tests to evaluate mechanical properties of carbon black particles after ageing



4 The change in mechanical properties of carbon black

- Carbon Black (CB) microstructure after ageing changes due to oil/additive chemical interactions.
- The crystallinity of aged CB was similar to soot extracted from used oil.
- CB particles exhibit size dependent elastic-plastic deformation under nanocompression tests.
- The mechanical properties of CB changes after ageing in the engine oil.
- The load required to deform/crack the CB after oil ageing increases significantly.

Probing the Mechanical Properties of Soot to Understand the Tribology of Contaminated Diesel Engine Oils

A. Al Sheikh Omar ^{a*}, F. Motamen. Salehi ^a, M. Bai ^{b,c}, B. J. Jnkson ^b & A. Morina ^a

menaals@leeds.ac.uk ^{a*}

^a University of Leeds, School of Mechanical Engineering, Institute of Functional Surfaces, Leeds, UK

^b University of Sheffield, Department of Materials Science and Engineering, Sheffield, UK

^c Centre for Manufacturing and Materials, Coventry University, Coventry, UK

Abstract

The study has evaluated the role of soot in affecting the performance of engine oils. It is very well known that the existence of soot in oil produces abrasive wear on the contact surfaces. Other mechanisms influence the oil performance such as additives adsorption on soot and oil degradation due to the interactions with soot. Recent research has suggested the existence of another wear mechanism related to soot particles, which remains poorly understood. This study investigates the effect of soot interactions in engine oil on its mechanical properties. Carbon black particles (CBPs) were used in the experiments to simulate real soot in the engine. The microstructure and crystal structure of CBPs compared to real soot were investigated using transmission electron microscopy (TEM) and X-ray diffraction (XRD). *In situ* compression of the single particle was conducted in a scanning electron microscope (SEM) to evaluate the mechanical properties of fresh and aged CBPs with different sizes (100-200 nm). The results show that aged CBPs are significantly harder than fresh CBPs, indicating that ageing in oil modifies the turbostratic crystal structure of soot and alters its mechanical properties, potentially affecting tribological performance.

Keywords

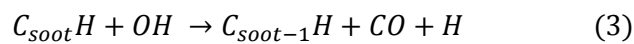
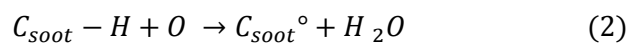
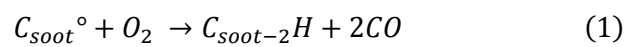
Soot, *In situ* SEM, Nanoindentation, Crystal structure, Mechanical properties, Tribology.

1. Introduction

Soot is identified as carbonaceous material (>90 % carbon) which is produced during the combustion process in the diesel engine [1], [2]. Several studies [1]–[3] have revealed that soot particles typically have a spherical shape with varied sizes from nanometres to aggregates in micrometres [1]–[3]. The crystal structure of soot consists of core and shell, which can vary from mostly amorphous or random in the core to the perfectly ordered crystalline structure of graphite in the shell [4]. Based on several studies [5]–[9], it was proposed that wear on contact surfaces is correlated to hard soot particles causing abrasive wear on the surfaces. The change in the crystal structure of soot could influence the

wear [1], [10]–[12]. Uy et al. [1] proved that different types of soot have different crystal structures influencing the hardness of particles and hence wear.

The correlation between the nature of soot and wear of contact surfaces is an interesting area in the lubricant industry. Understanding soot particles in terms of structure, morphology and mechanical properties under sliding or compression is a major issue to reduce the wear effects [4], [10]. Several studies [10], [11], [13], [14] have investigated the effect of soot interactions with oils' additives and bulk oil, causing additive adsorption and oil degradation. Salehi et al. [13] studied the absorption of ZDDP additive on soot particles. The authors proposed that additive adsorption on soot particles due to the high reactive surface of soot might cause a change in the hardness of particles. There are complex chemical interactions between the additives themselves and the soot in the existence of oxygen at high temperatures [11]. An increase in the soot surface area led to higher interaction between soot particles and additives accelerating the oil degradation [11]. The interaction between calcium phosphates, which is a detergent compound and considered a hard material in nature, and soot particles could change the abrasive characteristics of these particles [10]. The effect of soot on oil oxidation has shown that a higher level of soot in engine oil causes a higher oxidation rate [13], [14], which could influence the soot microstructure. Soot oxidation occurs when the soot particles react with O , O_2 and OH . Molecular Oxygen (O_2) plays the main role in this process due to plenty of O_2 . The main chemical reactions that contribute to soot oxidation are explained in equations (1), (2), and (3) [15], [16]. Several studies [17]–[23] reported the formation of an oxide layer around soot particles due to soot oxidation, which could potentially affect the mechanical properties of soot particles. Therefore, the interactions between the additives, oil and soot require more in-depth investigations to understand the exact evolution of the mechanical properties of soot particles using different oil/additive conditions.



Where; C_{soot}° is dehydrogenated sites on the soot.

The *in situ* TEM nanoindenter technique has been used in several works to identify the nanoscale mechanical properties of nanosize materials such as silicon nanowires [24], silicon nanospheres [15], [25], MoS₂ nanoparticles [26], ZnO nanowires [27] and carbon nanotubes [28]. Lahouij et al. [29] studied the mechanical properties of single and agglomerates of soot particles. Sliding and

compression tests were performed to investigate soot particles' behaviour using the *in situ* TEM nanoindenter technique. The results showed that soot in either single or agglomerate states resisted the applied deformation load. The single particle of soot under compression exhibited elastic-plastic behaviour after compression until 7 GPa contact pressure. Jenei et al. [30] performed *in-situ* compression tests in TEM to measure the mechanical properties of soot particles extracted from diesel engine oil. During the compression, the soot particles exhibited elastic-plastic behaviour and suffered permanent changes in the size and shape of their structure. The results showed an increase in calculated hardness and Young's modulus of the soot particles after consecutive compressions. Up to a contact pressure of 16 GPa no noticeable fracture was observed after compression, while the shape of soot particles was changed. The hardness of soot particles was registered in the range of 3-16 GPa, which is harder than ZDDP tribofilm (2-5 GPa) [30]. Bhowmick et al. [31] performed soot nano-indentation using an atomic force microscope (AFM). The findings demonstrated that a maximum load of 100 μ N was recorded to resist the indentation movement into the soot particles with no fracture observed. This study, for the first time, will investigate the effect of the change in the microstructure of soot on the mechanical properties of soot particles.

In this study, the mechanical properties of CB particles exposed to oil using in-situ compression testing inside a Scanning Electron Microscope (SEM) have been measured for the first time. The effect of the change in the crystal structure of CB after being ageing on its mechanical properties has been investigated and discussed.

2. Methodology

2.1 Materials and Methods

Carbon black particles (CBPs, Monarch120, Cabot Corporation, Massachusetts, USA) were used in this study to simulate the soot particles in engine oil. The diameter of a single CBP is less than 50 nm and the particles agglomerate in large clusters. Fully Formulated Oil (FFO) with a viscosity grade of 10W-40 was used in the diesel engine environment. FFO consists of synthetic base oil and several additives including anti-wear additive, dispersant, detergent, and antioxidant additives. The oil containing 1.5 wt% CB has been artificially aged in the lab for 96 hrs in accordance with ASTM D4636-99 standard [32]. The ageing period is chosen according to the D4636 standard [33], which allows measurable results (e.g. oxidation) to be obtained in a reasonable time [33]. The ageing method was described in detail in our previous papers [34], [35].

2.2 Nanoparticles extraction from the oil

The CB and real soot particles were extracted from the aged oil and used oil using a centrifuge (Thermo Scientific Heraeus Megafuge 16R) at speed of 12000 rpm for 2 hrs. To remove the oil from the particles' surfaces after centrifugation, the particles were washed with heptane and centrifuged again as demonstrated in Figure 1. Finally, the particles were dried in an oven overnight at 40 °C for further analysis.

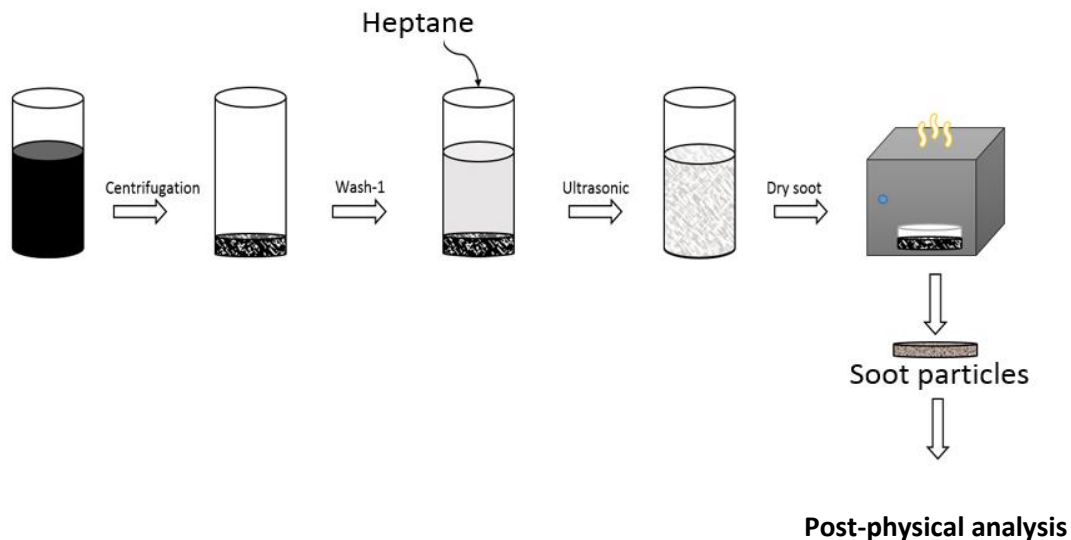


Figure 1: Diagram of the extraction process of CB/soot particles from the aged oil.

2.3 *In situ* SEM nanoindentation

An in-situ nanoindenter system (Alemnis AG, Thun, Switzerland) equipped with a 60° conical diamond tip (tip diameter 0.7 μm, SYNTON-MDP AG, Switzerland) was used inside a FEG-SEM (FEI, Nova NanoSEM 450) for the compression test of a single particle (Figure 2a,b). The force-displacement curve was recorded together with the SEM imaging of the particle deformation during the indentation process. The particles were first dispersed in iso-propanol using an ultrasonic bath for two minutes, and then a droplet was spread on a silicon single-crystal wafer and dried overnight. Nanoparticles were found to stick on the wedge surface by Van der Waals forces (Figure 3).

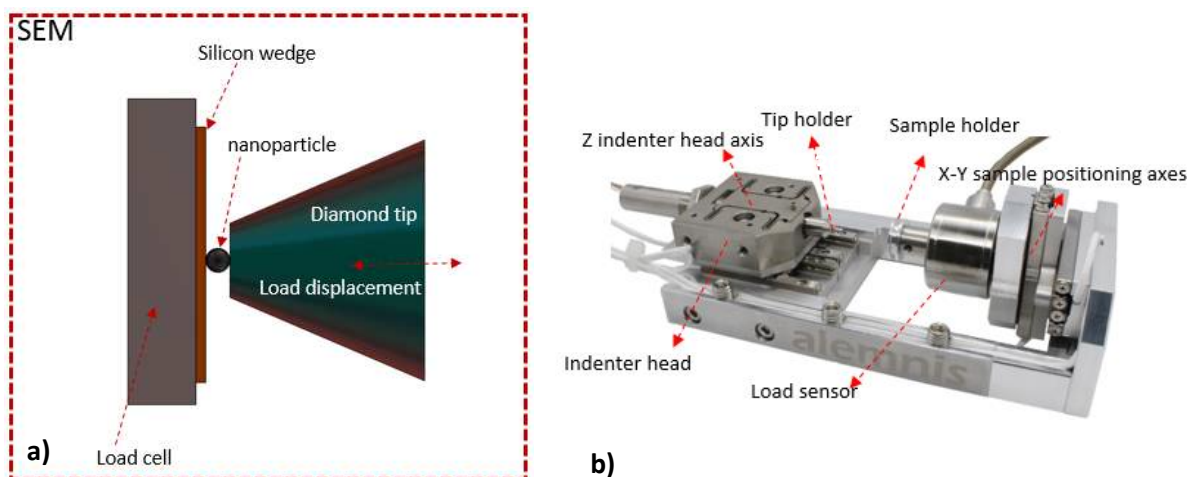


Figure 2: (a) Schematic representation of nanoindenter performing a compression test on soot particle in the SEM (b) Alemnis nanoindenter.

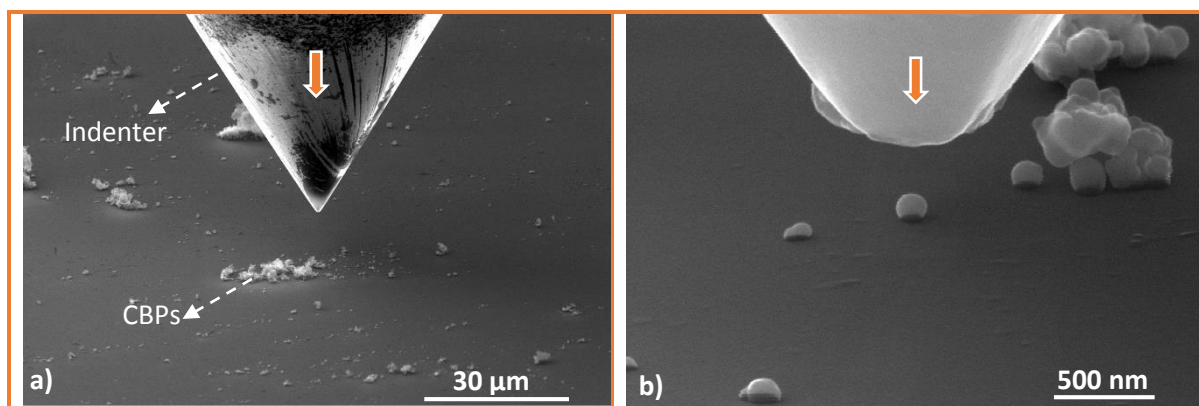


Figure 3: (a) *In situ* nanoindentation of CBPs on a Si surface, (b) The diamond indenter is approaching the targeted particle for compressing.

2.4 Crystal structure analysis

Transmission Electron Microscopy (TEM, FEI Titan Themis Cubed 300) was used in this study to analyse the crystal structure of a small number of CBP/soot nanoparticles at the high spatial resolution, using E-beam energy of 120 keV, with 0.2 eV energy spread.

X-ray Diffraction (XRD, Bruker D8, Germany) was used to identify the crystallographic structure of the crystal structure of CB and soot particles. The scan angle (2θ) ranged between 10 to 90°. The X-ray generator of this technique was 2 KW. Maximum angular speed is 15 °/sec. In this study, the two peaks at 2θ positions $\sim 25^\circ$ and 43° are indexed as the (002) and (100) graphite-type reflections respectively arising from the turbostratic carbon structure [10], [36], [37].

3. Results

3.1 Physical characterisation of CB and soot

3.1.1 TEM crystal structure

TEM was used to investigate the crystal structure of fresh and aged CB compared to real soot particles. Aged CB and soot particles were extracted from aged oil and used oil respectively by centrifugation. TEM images were captured for 20 different CB clusters (fresh and aged). The crystal structure of primary CB particles (fresh and aged) consists of the inner core and outer shell (Figure 4a, b, c and d). The shell thickness of as-received CB particles (fresh and aged) is approximately ≤ 7 nm. The CB shell displays graphene sheets arranged concentrically around the core. The internal structure of CB particles reveals turbostratic domains with randomly oriented graphene platelets. TEM images of aged CB particles show the formation of an additional thin layer outside the shell with a thickness of ≤ 3 nm (Figure 4c, d).

A similar layer was found around the outer soot shell in previous studies [18], [19]. Some studies [17], [18] reported that large particles with a higher degree of crystallinity can block O_2 diffusion through their outer shell. They proposed that O_2 diffusion into the core is only possible for small particles since for larger particles O_2 atoms react with edge-site atoms of shell particles. The passivated shell does not allow O_2 to access and diffuse through to the reactive amorphous core [18]. This causes the formation of an oxidation layer on the outer shell of aged CB.

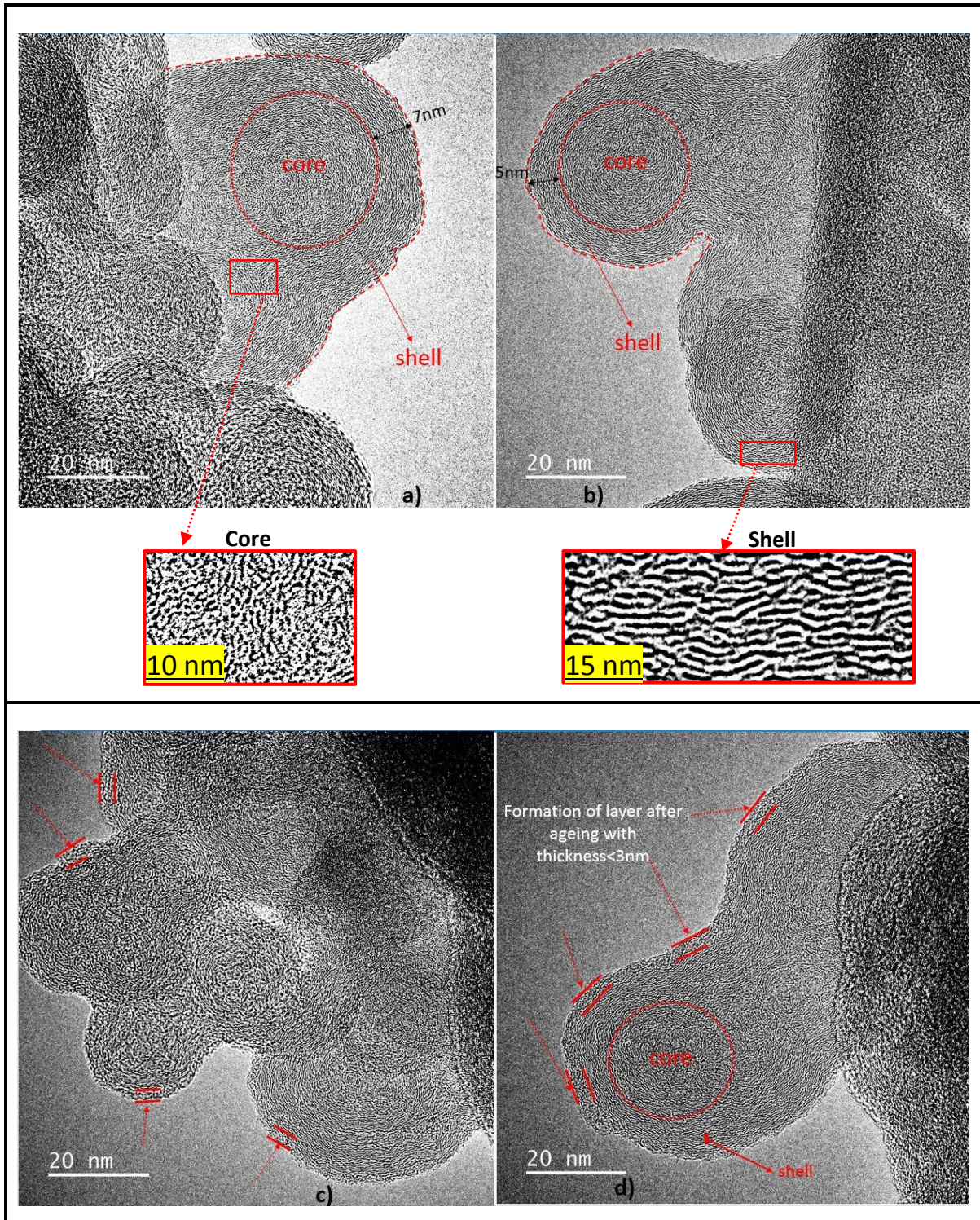


Figure 4: TEM images of a), b) fresh CB primary particles and c), d) aged CB primary particles.

The microstructures of the fresh and aged CB particles (Figure 4) were compared to the soot particles extracted from used oil (Figure 5). The crystal structure of soot consists of core and shell (Figure 5a and b). TEM images of CB and soot particles show to have similar crystal structure. The graphitic shell thickness of soot subparticles varies and reaches up to 10 nm in some particles as shown in Figure 5a,b. The soot particles investigated displayed an amorphous layer surrounding the shell with a

thickness of less than 2 nm. This thin layer looks similar to the amorphous layer found after ageing CB in the same oil (Figure 4c and b). This is in line with several studies [17]–[19] reported an amorphous layer surrounded the shell as a result of soot oxidation. The layer surrounding the soot shell could also contain impurities originating from soot interactions with oil additives at high temperatures. Pal et al [38] investigated soot oxidation *in situ* and in real-time. The results demonstrated that soot oxidation occurred not only for the particles' surface but also for the internal soot particles that were oxidised.

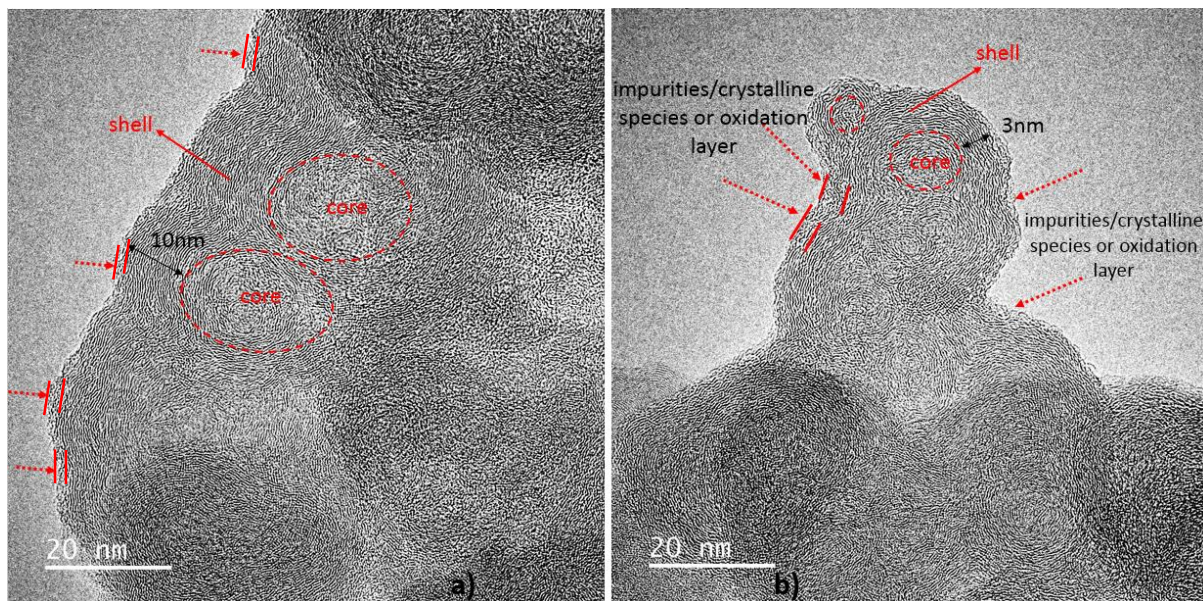


Figure 5: TEM images (a, b) of the primary soot particles extracted from used oil.

3..1.2 XRD crystal structure

XRD technique was employed to identify the internal crystalline structure of CB, and the effect of the ageing process on the internal structure of CB. TEM results focused on a tiny part of the materials due to the extremely high magnification applied. Thus, the XRD technique was used to get a clear picture of bulk materials, which are usually combinations of many crystallites, particles and other nano-objects. The obtained data about the atomic structure are averaged over the whole sample volume under the probe [36]. In this study, fresh CB, and particles extracted from the oil, including the aged CB, and soot particles, were investigated using the XRD technique. The XRD information was recorded for the entire scan range of 10-90 ° θ as shown in Figure 6.

The X-ray diffraction patterns are composed of two broad peaks at $\sim 25^\circ$ and 43° , (Figure 6) indexed as the (002) and (100) graphite-type reflections respectively [36], [37]. These two peaks are consistent with the turbostratic carbon structure [36], [37]. TEM images in this study confirmed the turbostratic structure for CB (fresh and aged) and soot.

XRD result of CB after ageing (Figure 6b,c) displays a change in peak width (dispersive shoulder peak ranging from 15° to 21.5°). XRD data of aged CB is similar to the study that showed defects of CB atomic [39]. In this study, CB was aged at a high temperature in the presence of additives and oxygen, which influence the CB structure. XRD data of the oxidation of graphite in oils at the same 2 θ orientation was investigated by Gupta et al. [40]. The shoulder at 2 θ of 15° to 21.5° in graphite oxide results [40] is similar to aged CB data in this study. This correlated to the intercalation of oxygen groups that existed in the oil causing oxidation of graphite. Other studies [19], [41] found that the existence of oxygen causes soot oxidation for surface particles and the internal structure. In this study, both TEM and XRD results proved the change of CB crystal structure after ageing CB in the oil.

Figure 6a reveals the crystal structure of soot extracted from the used oil compared to fresh CBP and aged CBP. Similar to fresh and aged CBP analysis, two main peaks at 2 θ positions ~25° and 43° are observed in the soot XRD spectrum (Figure 6a). The small sharp peaks (A, B, C and D) represent various crystalline species, or impurities such as calcium-based compounds, which can also precipitate within oil [10], [42]. These peaks (A, B, C and D) indicate that various crystalline species were embedded into turbostratic carbonaceous soot. A similar XRD spectrum of soot analysis (Figure 6a) was investigated by Sharma et al. [10], [42]. XRD data of soot showed a dispersive shoulder peak ranging from ~15° to 21.5° which is similar to the aged CB spectrum (Figure 6b). Dispersive shoulder peak reveals the oxidation of soot particles [40]. The results are in line with TEM images (Figure 5) that confirmed the change in the crystal structure of CB particles after ageing is similar to the soot extracted from used oil.

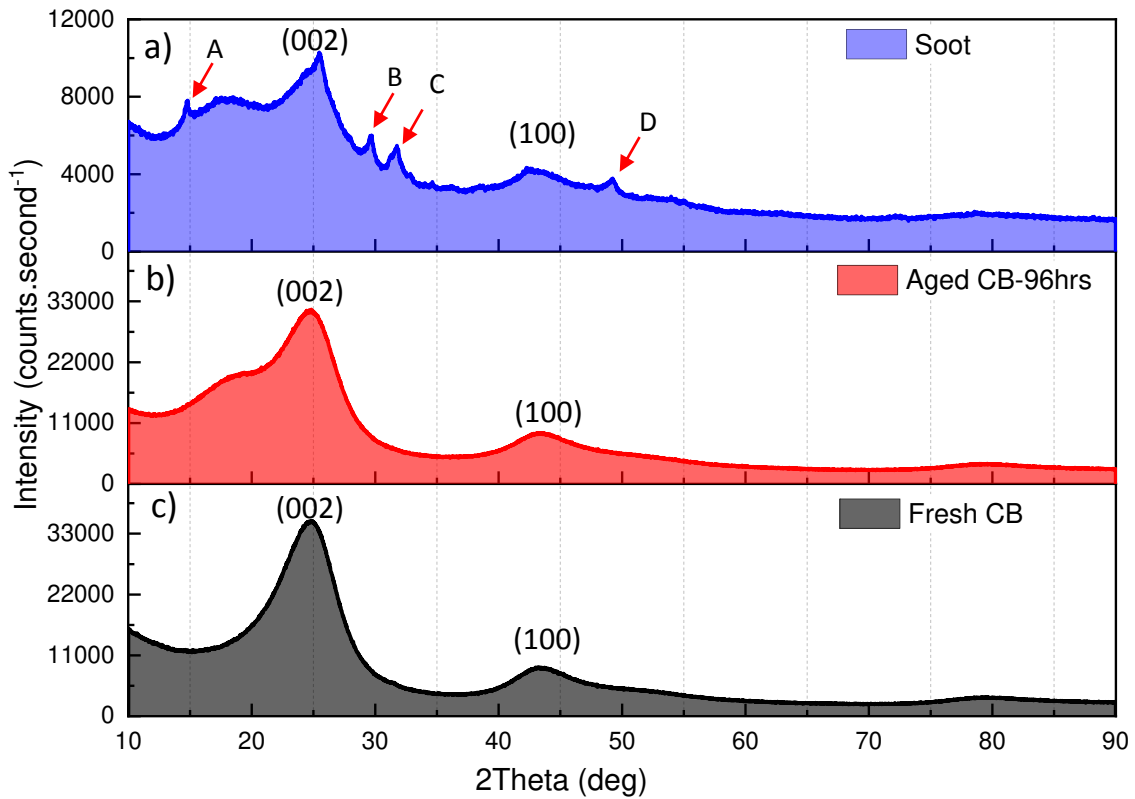


Figure 6: XRD results of the crystal structure of soot (a), aged CB-96hrs (b) and fresh CB (c). The small sharp peaks A, B, C and D represent various crystalline species or impurities.

3.2 *In situ* nanoindentation of CBP

3.2.1 Nanocompression of fresh CBP

To evaluate the mechanical properties of individual CB particles, *in situ* nanoindentation experiments of fresh CB were performed at two different particle sizes (130-140 nm and 200-240 nm). Figure 7d demonstrates the recorded load-displacement curve after compressing a 200-240 nm CBP with a diamond tip (Figure 7a). The CBP particle cracked after approximately 70 nm compressing displacement, at an applied load of 100 μN (called fracture load). The visible surface crack (Figure 7c) caused a drop in load of 60 μN , but the compressed CBP did not fail completely. Continued indentation of the deformed particle and Si substrate increased the applied load to 120 μN . The CB particle under compression undergoes elastic-plastic deformation. In this study, it was difficult to calculate the

hardness of the particles due to the unknown contact area during compression, however the fracture load can be assessed *in situ*.

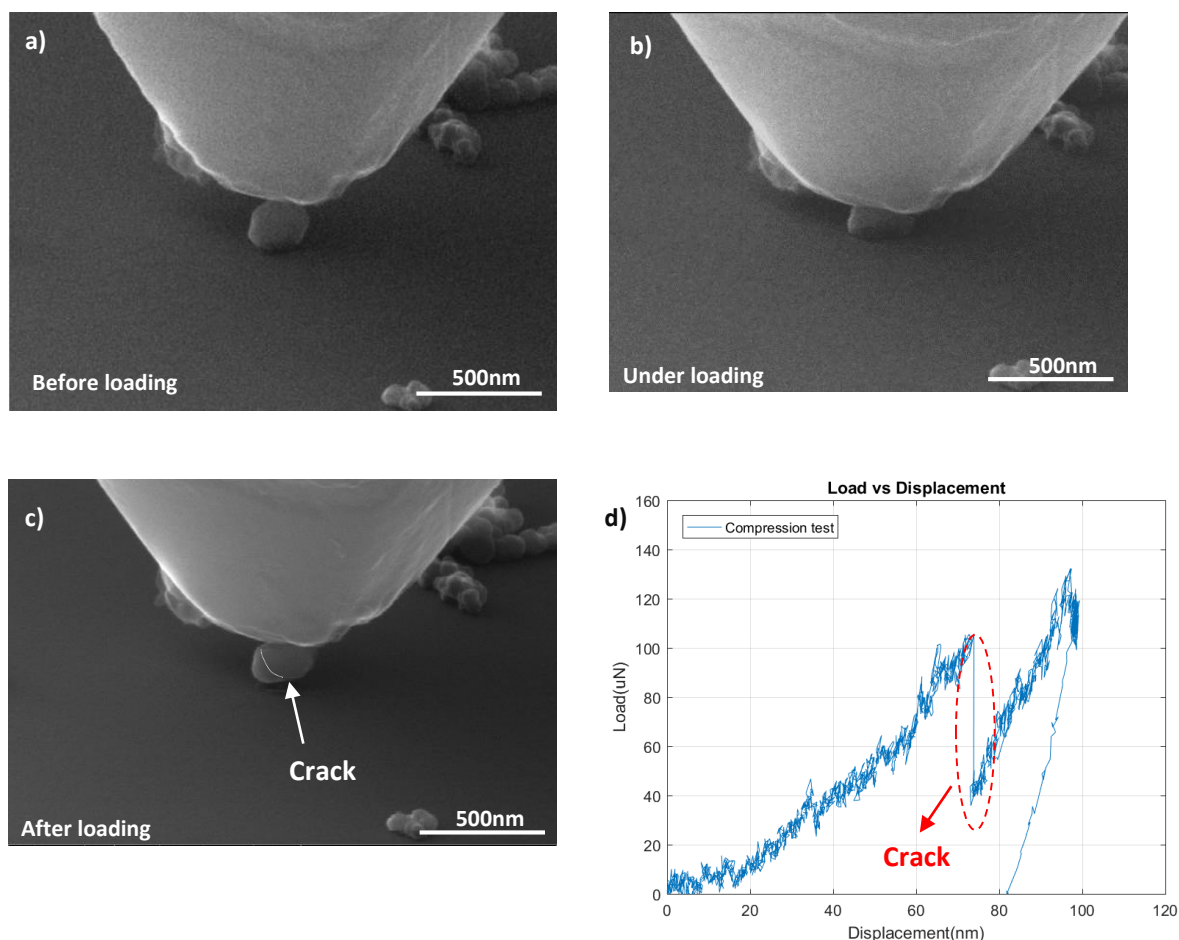


Figure 7: Nanocompression test of fresh CB particle of size 200-240 nm (a) before loading, (b) under loading, (c) after loading, (d) load-displacement curve.

In situ nanocompression test was carried out to investigate the deformation of a smaller CB particle with a size of (130-140 nm) (Figure 8a). The corresponding load-displacement curve reveals deformation in the CB particle after approximately 40 nm compressing displacement corresponding to 20 μN applied load (Figure 8a). The CB particle after compression is oblate (Figure 8b). Similar to the (200-240 nm) compression test, the increase in the load after deforming the CBP was correlated to continued indentation into the Si substrate underneath the particle (Figure 8b). Figure 8a compares the deformation force to plastically deform the CBP at different particles sizes (130-140 nm and 200-240 nm). The results show that the larger CBP has higher fracture load compared to the smaller CBP (130-140 nm). The load of the larger particle is 100 μN compared to 25 μN of the smaller CBP.

It is important to note that the compaction of the particles and silicon substrate is partially reversible (Figure 8a). Lahouij et al [29] studied nanocompression of soot particles using a TEM nanoindenter.

The findings showed that soot particles deform when the contact pressure is above 7 GPa. The soot particles exhibited elastic-plastic behaviour. Bhowmick et al [31] determined the maximum applied load on soot particles using nanoindentation. The results demonstrated that the maximum applied load on the soot particle is 100 μN before the deformation in the soot particle occurred [31].

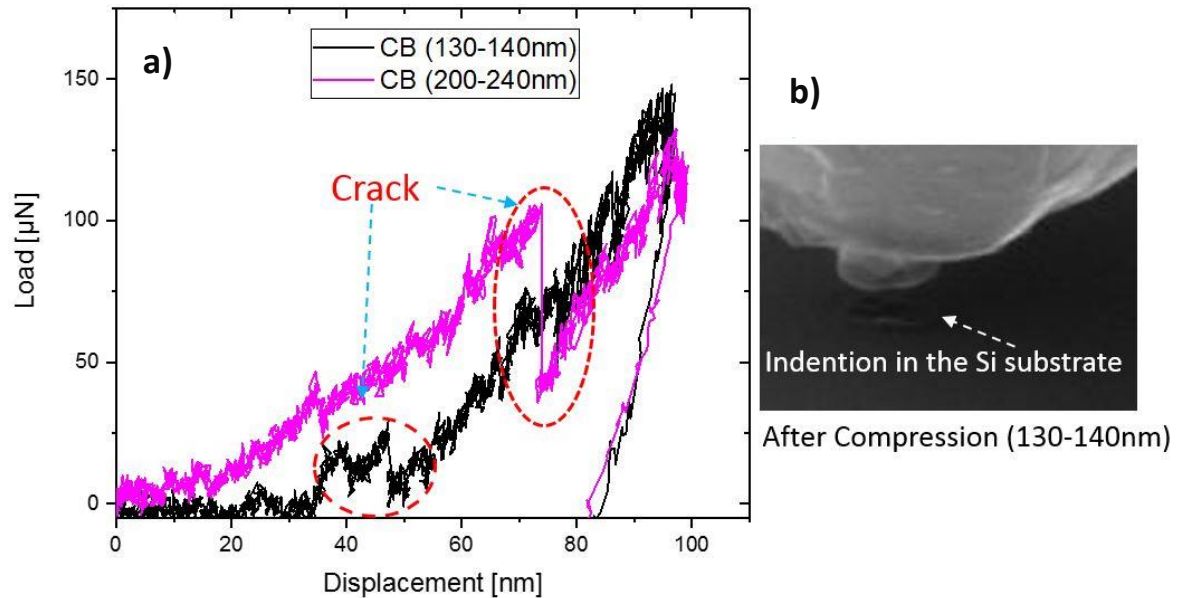


Figure 8: (a) Nano-compression tests of fresh CBP by diamond at different particles size, (b) Residual indentation in Si substrate after compressing a (130-140 nm) particle.

3.2.2 Nanocompression of aged CBP

In-situ nanocompression of the aged CBP at different sizes (130-140 nm) and (210-220 nm) were performed to investigate the effect of the ageing process in oil on the mechanical properties of CBP. The corresponding load-displacement curve of the 210-220 nm particle compression test is shown in Figure 9d. During the compression process (Figure 9b), the applied load increases progressively until particle deformation occurs approximately at 200 μN (90 nm compressing displacement). After the

compression test, a surface crack running vertically from the contact zone can be observed in the aged CB particle (Figure 9c), consistent with the load drop observed.

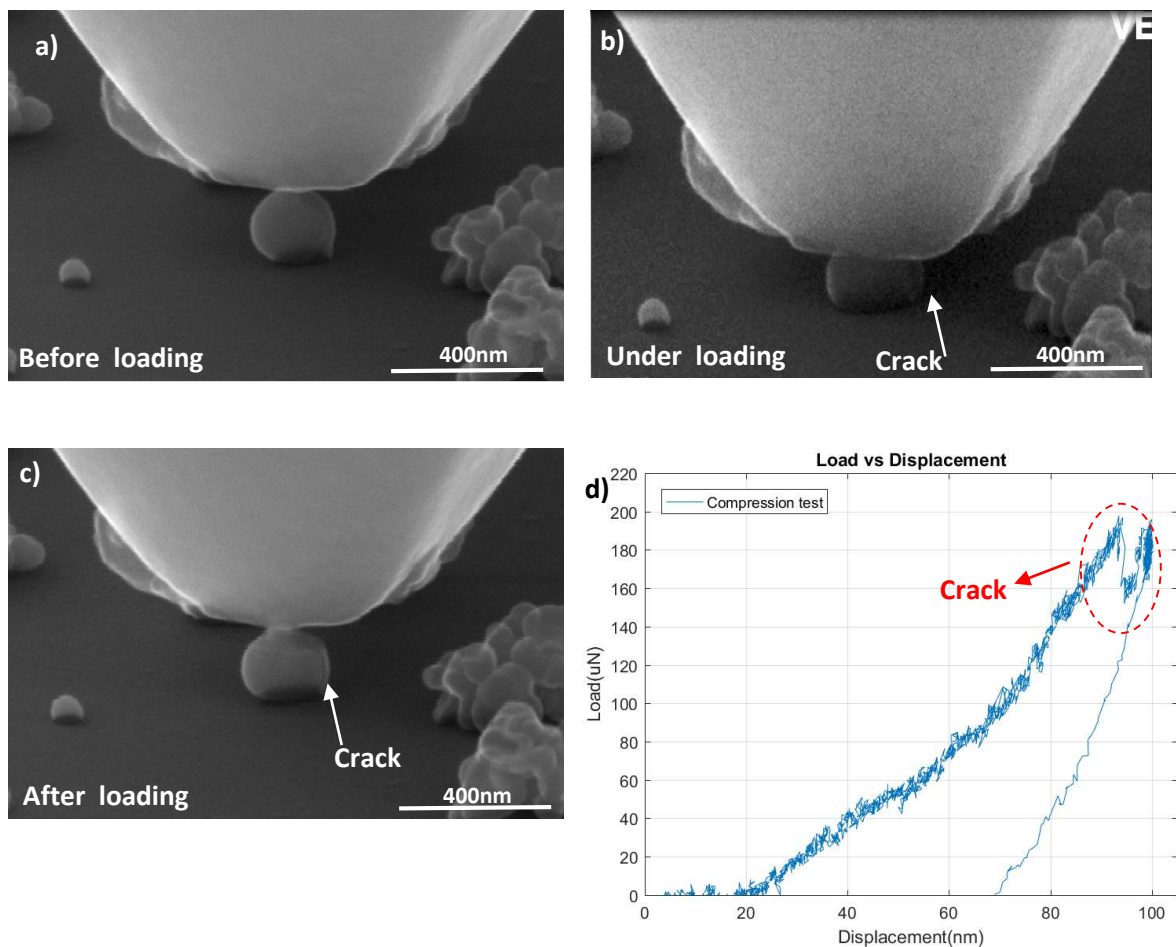


Figure 9: Nano-compression test aged CBP at size (210-220 nm) (a) before loading, (b) under loading, (c) after loading, (d) load-displacement curve.

The load-displacement curves of two different sizes of aged CB particles (130-140 nm) and (210-220 nm) are compared in Figure 10(a). The larger aged-CB particle (210-220 nm) required a higher load to deform the particle compared to the smaller aged-CB particle (130-140 nm). Similar to fresh CB, the larger particle has more resistance to deform compared to smaller CBP, and the observed deformation was the initiation of a radial crack propagating from the indenter contact zone across the CBP surface. The aged-CB particle (130-140 nm) was deformed and oblate after compression as shown in Figure 10b, and compressed Si substrate underneath the particle (Figure 10a,b). The fracture load of the larger aged-CB particle is 200 μN compared to 100 μN of the smaller aged-CB particle. The results

demonstrate that the aged-CB particle under nanocompression also undergoes elastic-plastic deformation.

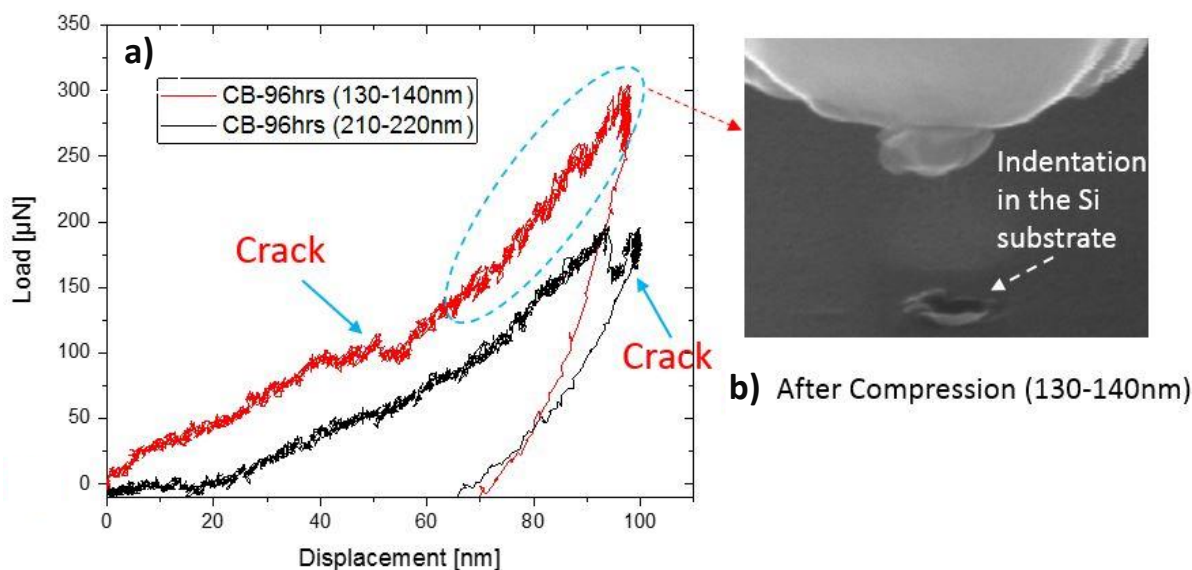


Figure 10: Nanocompression tests of aged CBP at different particles sizes, b) indentation in the Si substrate after compressing 130-140 nm particle.

4. Discussion

It has been proposed that the mechanical properties of soot particles are changed in oil at different conditions leading to an increase in wear [31]. Bhowmick et al. [31] and Sharma et al. [10] suggested that chemical interactions between soot and additives could change the abrasive characteristics of these particles [10]. Our previous study [11] showed the existence of CB in the oil at ageing conditions induced oil oxidation due to the chemical interaction between the CB surface and additives. Other studies [17]–[23], [38], [41] reported the formation of an oxidation layer around soot particles and internal soot oxidation which could affect the mechanical properties of soot particles. However, there is no evidence to support this hypothesis. This study, for the first time, has investigated the effect of the change in the microstructure of soot on the mechanical properties of soot particles.

In this study, TEM images (Figure 4c, d) and XRD data (Figure 6) proved that the crystal structure of CB changes after ageing in oil. TEM images (Figure 4c, d) showed the formation of a layer with a thickness of ≤ 3 nm around aged CB particles. The comparison between the crystal structure of soot and aged CBP demonstrated that the CBP crystal structure is similar to soot. The change in the crystal structure of soot/CB particles after ageing resulted from the oxidation of the soot/CB surface [38], [41]. The O_2 diffuses through the outer shell of the particles to react with edge-site atoms of shell particles. The passivated shell did not allow O_2 to access and diffuse through the reactive amorphous core forming

the oxidation layer on the outer shell of CB or soot [20]–[23]. The results are in line with other studies that demonstrated the formation of the oxidation layer around soot particles [17]–[23], [38]. While other studies [19], [38], [41] found that internal soot particles were also oxidized causing the change in the microstructure of soot.

The *in situ* SEM nanoindentation of CB revealed that the applied load required to initiate significant plastic deformation of CB after ageing increased significantly for particles in two different sizes (Figure 11). The increase in the deformation load correlates with a higher particle hardness, meaning a higher compressive load is required to deform/break the CB particles after ageing in the oil. The hardness of the CB is increased due to the change in the crystal structure of CB particles after ageing. A higher deformation load was required to deform the larger particle for both aged and fresh CB.

The results are in the line with other studies [1], [10], [31] that proposed the change in mechanical properties of soot after ageing. This is the first study that has investigated the relationship between the change in the crystal structure of CB after ageing in the oil and the mechanical properties of CB. These findings are in line with Uy et al. [1] who showed that different types of soot, extracted from various oils, had different morphology which could affect the hardness of particles and hence the wear. The findings in this study support other studies [5]–[9] proposed that changes in the crystal of soot particles due to interactions with additives influence the mechanical properties of soot and hence wear [1], [10]–[12].

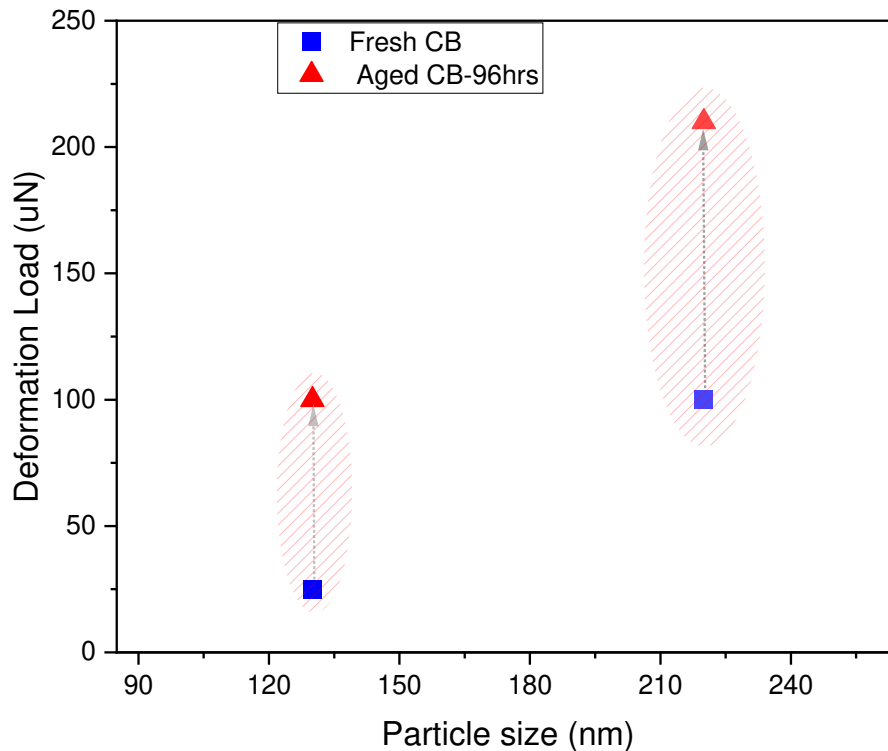


Figure 11: Deformation load of CB after ageing in oil for two different particles sizes. The deformation load was measured *in situ* at the point where the CB particles were deformed/cracked during nano-compression tests.

5. Conclusions

In this current study, the change in CBPs microstructure after interactions in engine oil under ageing conditions has been investigated. It has previously been reported that soot/CB can adsorb oil additives and induce oil degradation which influence wear. However, no experimental studies have addressed the effect of soot evolution in the oil, and on its microstructure which could influence the mechanical properties of soot particles. It is worth noting that the changes in the mechanical properties of soot particles could affect the wear. The following conclusions are summarised:

- The microstructure of CBP after ageing in engine oil was changed with the formation of a thin amorphous layer around the particles.
- The crystallinity of aged CBP (measured by XRD) was similar to soot extracted from used oil except some additional impurities were found on soot particles.
- CB particles before and after ageing exhibited size dependent elastic-plastic deformation under nanocompression tests. Larger particles exhibited surface cracking.

- For a given particle size, nano-compression experiments revealed that the load required to deform/crack the CBP after oil ageing was approximately double compared to that for pristine CBP, indicating substantial hardening.
- The findings proved for the first time that the change in CB microstructure due to oil/additive chemical interactions causes a change in the mechanical properties of CBP.

6. Acknowledgements

The authors would like to thank Parker Hannifin Ltd and the EPSRC Centre for Doctoral Training for Integrated Tribology for providing the fund for this research. Grant No. EP/I01629X/1. This work is supported by the Engineering and Physical Sciences Research Council (Grant number EP/R001766/1) as a part of 'Friction: The Tribology Enigma' (www.friction.org.uk), a collaborative Programme Grant between the Universities of Leeds and Sheffield.

The authors would like to pay their gratitude and respects to Professor Anne Neville who passed away in July of 2022. Anne contributed to establishing the research programme presented in this paper.

7. Declaration of Interest Statement

There are no conflicts of interest.

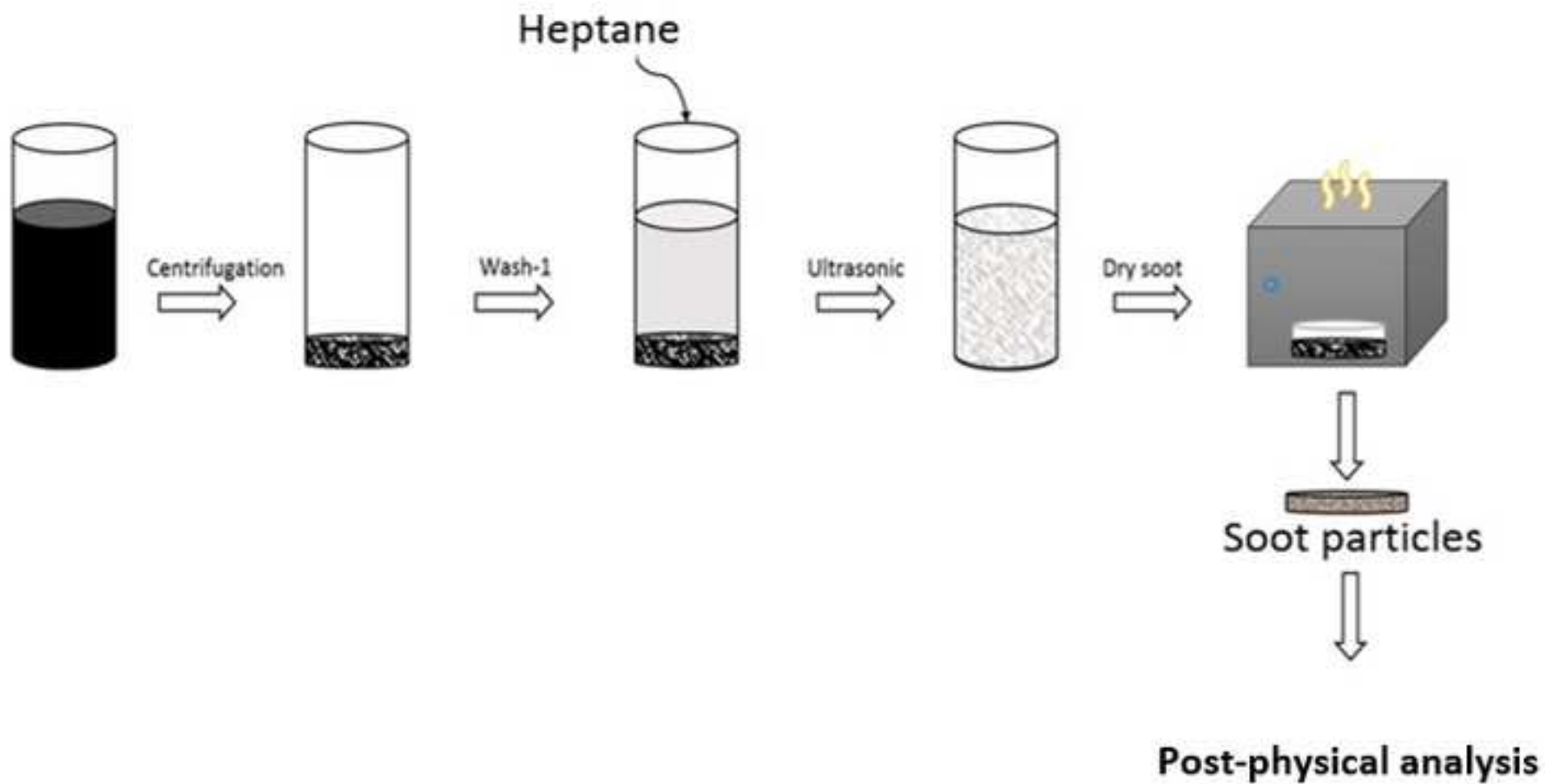
8. References

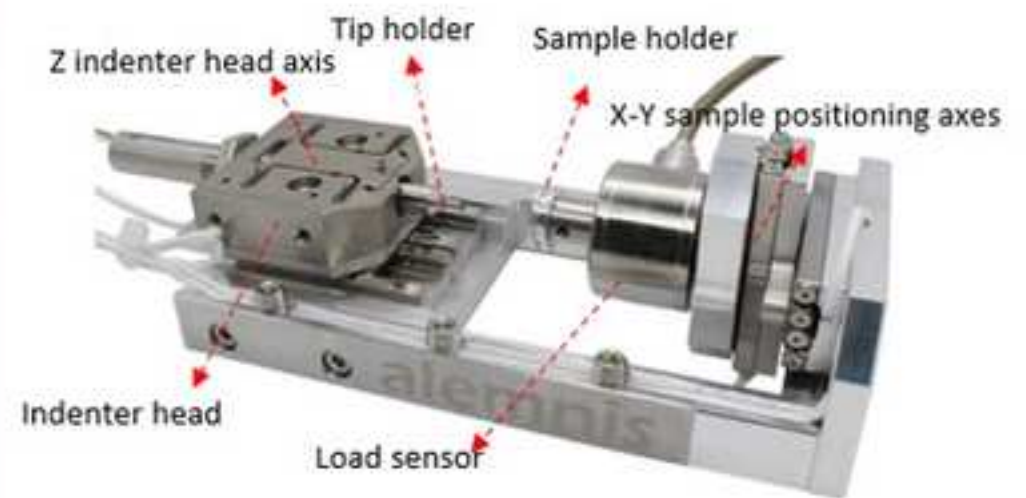
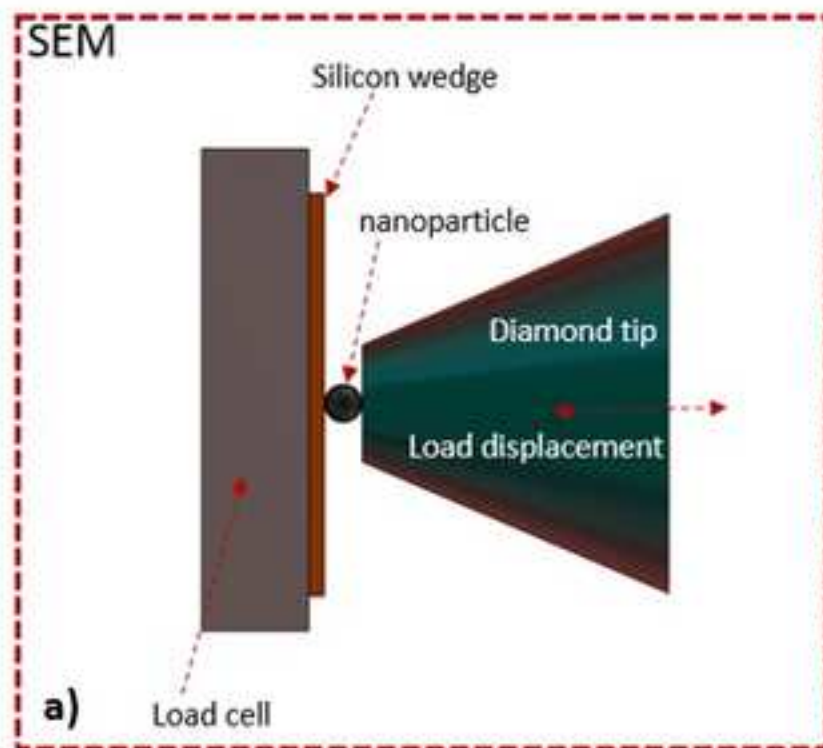
- [1] D. Uy *et al.*, "Characterization of gasoline soot and comparison to diesel soot: Morphology, chemistry, and wear," *Tribol. Int.*, vol. 80, pp. 198–209, 2014.
- [2] V. Sharma *et al.*, "Structure and chemistry of crankcase and exhaust soot extracted from diesel engines," *Carbon N. Y.*, vol. 103, pp. 327–338, 2016.
- [3] B. A. A. L. van Setten, M. Makkee, and J. A. Moulijn, "Science and technology of catalytic diesel particulate filters," *Catal. Rev.*, vol. 43, no. 4, pp. 489–564, 2001.
- [4] H. Bhowmick and S. K. Biswas, "Relationship between physical structure and tribology of single soot particles generated by burning ethylene," *Tribol. Lett.*, vol. 44, no. 2, pp. 139–149, 2011.
- [5] C. C. Kuo, C. A. Passut, T.-C. Jao, A. A. Csontos, and J. M. Howe, "Wear mechanism in Cummins M-11 high soot diesel test engines," *SAE*, vol. 107, pp. 499–511, 1998.
- [6] D. A. Green, R. Lewis, and R. S. Dwyer-Joyce, "Wear effects and mechanisms of soot contaminated automotive lubricants," *Proc. Inst. Mech. Eng. Part J J. Eng. Tribol.*, vol. 220, no. 3, pp. 159–169, 2006.
- [7] F. Chinas-Castillo and H. A. Spikes, "The behavior of diluted sooted oils in lubricated contacts," *Tribol. Lett.*, vol. 16, no. 4, pp. 317–322, 2004.
- [8] D. A. Green and R. Lewis, "The effects of soot-contaminated engine oil on wear and friction: A

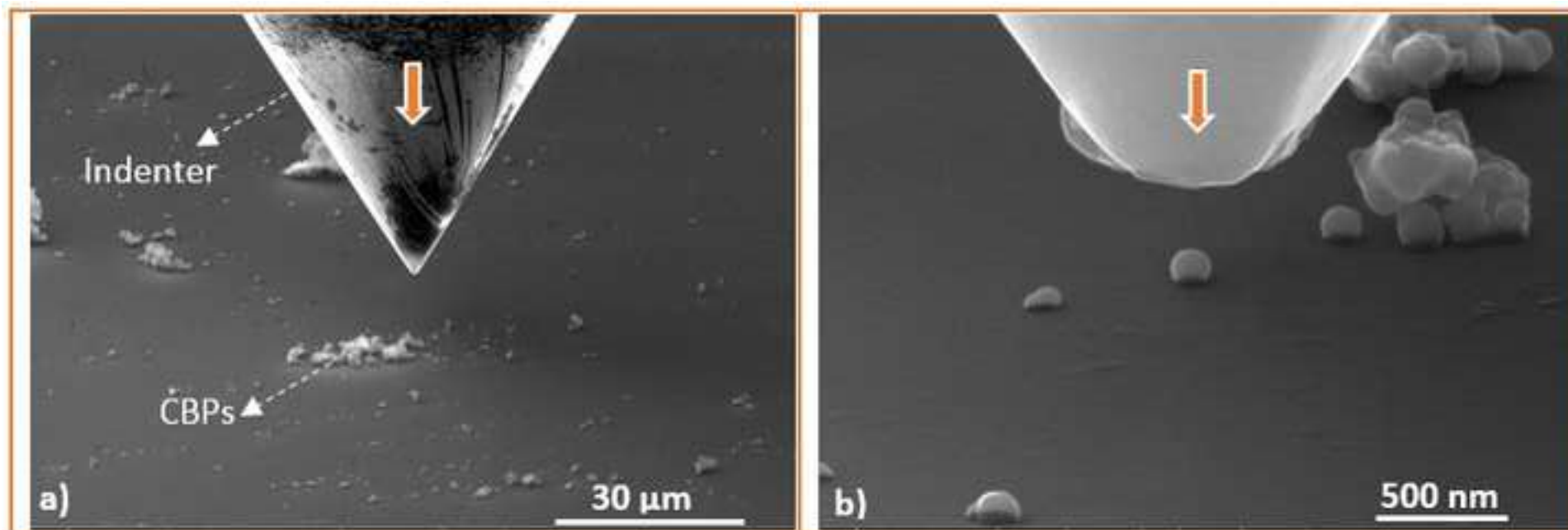
- review," *Proc. Inst. Mech. Eng. Part D J. Automob. Eng.*, vol. 222, no. 9, pp. 1669–1689, 2008.
- [9] Y. Gallo, "Late Cycle Soot Oxidation in Diesel Engines," Lund University, 2016.
- [10] V. Sharma, S. Bagi, M. Patel, O. Aderniran, and P. B. Aswath, "Influence of Engine Age on Morphology and Chemistry of Diesel Soot Extracted from Crankcase Oil," *Energy and Fuels*, vol. 30, no. 3, pp. 2276–2284, 2016.
- [11] A. Al Sheikh Omar, F. Motamen Salehi, U. Farooq, A. Morina, and A. Neville, "Chemical and physical assessment of engine oils degradation and additive depletion by soot," *Tribol. Int.*, vol. 160, no. April, p. 107054, 2021.
- [12] F. Motamen Salehi, A. Morina, and A. Neville, "Zinc Dialkyldithiophosphate Additive Adsorption on Carbon Black Particles," *Tribol. Lett.*, vol. 66, no. 3, p. 0, 2018.
- [13] F. Motamen Salehi, A. Morina, and A. Neville, "Zinc Dialkyldithiophosphate Additive Adsorption on Carbon Black Particles," *Tribol. Lett.*, vol. 66, no. 3, p. 0, 2018.
- [14] R. Penchaliah, T. J. Harvey, R. J. K. Wood, K. Nelson, and H. E. G. Powrie, "The effects of diesel contaminants on tribological performance on sliding steel on steel contacts," vol. 225, pp. 779–797, 2011.
- [15] A. L. Barnes, A. Morina, R. E. Andrew, and A. Neville, "The Effect of Additive Chemical Structure on the Tribofilms Derived from Varying Molybdenum-Sulfur Chemistries," *Tribol. Lett.*, vol. 69, no. 4, pp. 1–21, 2021.
- [16] "Ref12_Turns.Pdf." .
- [17] K. Kamegawa, K. Nishikubo, and H. Yoshida, "Oxidative degradation of carbon blacks with nitric acid (I) - Changes in pore and crystallographic structures," *Carbon N. Y.*, vol. 36, no. 4, pp. 433–441, 1998.
- [18] H. Ghiassi, P. Toth, I. C. Jaramillo, and J. A. S. Lighty, "Soot oxidation-induced fragmentation: Part 1: The relationship between soot nanostructure and oxidation-induced fragmentation," *Combust. Flame*, vol. 163, pp. 179–187, 2016.
- [19] A. D. Sediako, A. Bennett, W. L. Roberts, and M. J. Thomson, "In Situ Imaging Studies of Combustor Pressure Effects on Soot Oxidation," *Energy and Fuels*, vol. 33, no. 2, pp. 1582–1589, 2019.
- [20] R. H. Hurt, A. F. Sarofim, and J. P. Longwell, "Gasification-induced densification of carbons: From soot to form coke," *Combust. Flame*, vol. 95, no. 4, pp. 430–432, 1993.
- [21] F. A. Heckman, "Microstructure of carbon black," *Rubber Chem. Technol.*, vol. 37, no. 5, pp. 1245–1298, 1964.
- [22] J. B. Donnet, J. Schultz, and A. Eckhardt, "Etude de la microstructure d'un noir de carbone thermique," *Carbon N. Y.*, vol. 6, no. 6, pp. 781–788, 1968.
- [23] K. Kamegawa, K. Nishikubo, and H. Yoshida, "Oxidative degradation of carbon blacks with nitric acid (I)—Changes in pore and crystallographic structures," *Carbon N. Y.*, vol. 36, no. 4, pp. 433–441, 1998.
- [24] X. Han, K. Zheng, Y. Zhang, X. Zhang, Z. Zhang, and Z. L. Wang, "Low-temperature in situ large-strain plasticity of silicon nanowires," *Adv. Mater.*, vol. 19, no. 16, pp. 2112–2118, 2007.
- [25] J. Deneen, W. M. Mook, A. Minor, W. W. Gerberich, and C. B. Carter, "In situ deformation of silicon nanospheres," *J. Mater. Sci.*, vol. 41, no. 14, pp. 4477–4483, 2006.

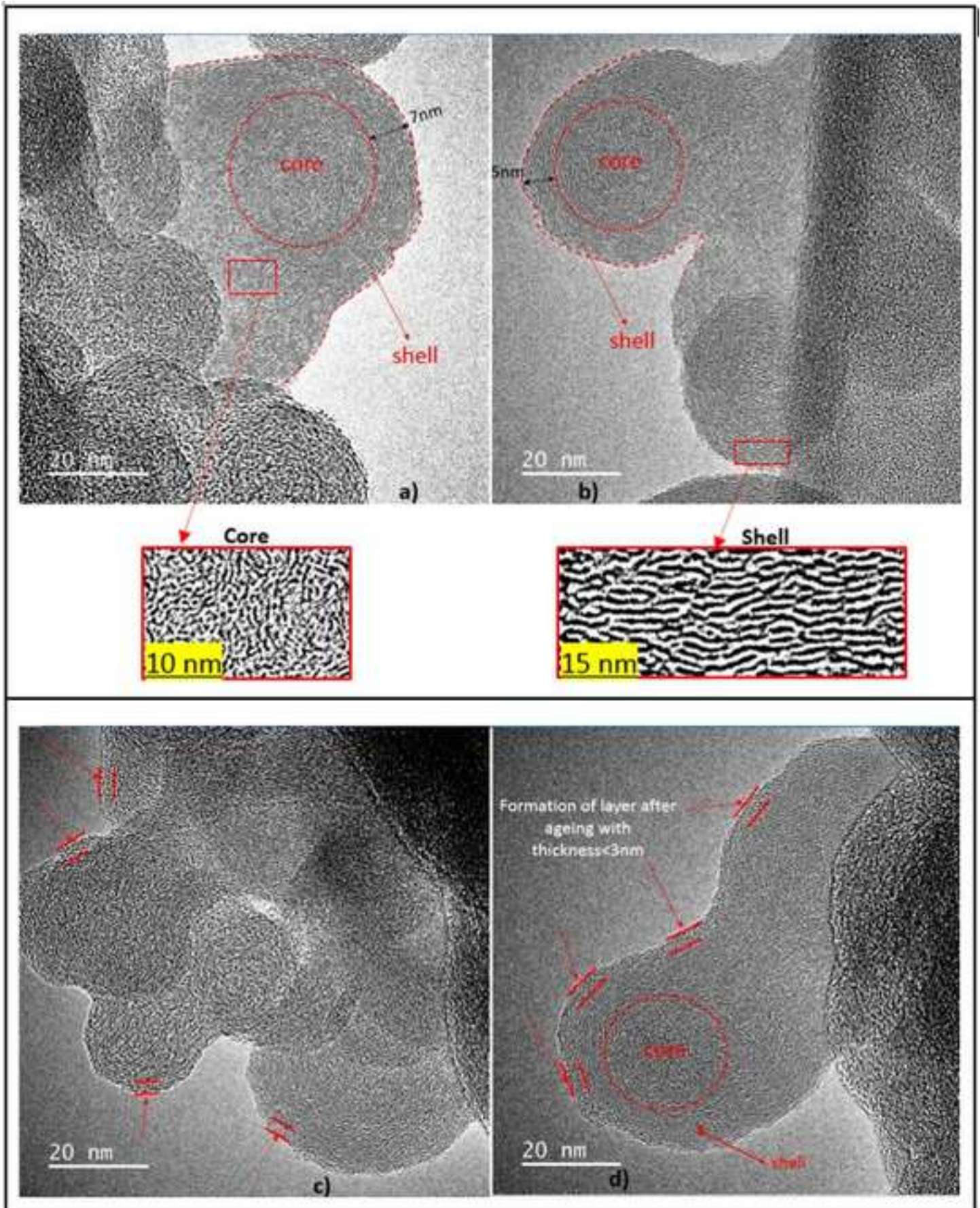
- [26] I. Lahouij, F. Dassenoy, B. Vacher, and J. M. Martin, "Real time TEM imaging of compression and shear of single fullerene-like MoS₂nanoparticle," *Tribol. Lett.*, vol. 45, no. 1, pp. 131–141, 2012.
- [27] A. Asthana, K. Momeni, A. Prasad, Y. K. Yap, and R. S. Yassar, "In situ observation of size-scale effects on the mechanical properties of ZnO nanowires," *Nanotechnology*, vol. 22, no. 26, 2011.
- [28] Z. L. Wang, P. Poncharal, and W. A. De Heer, "Measuring physical and mechanical properties of individual carbon nanotubes by in situ TEM," vol. 61, pp. 1025–1030, 2000.
- [29] I. Lahouij, F. Dassenoy, B. Vacher, K. Sinha, D. A. Brass, and M. Devine, "Understanding the deformation of soot particles/agglomerates in a dynamic contact: Tem in situ compression and shear experiments," *Tribol. Lett.*, vol. 53, no. 1, pp. 91–99, 2014.
- [30] I. Z. Jenei *et al.*, "Mechanical characterization of diesel soot nanoparticles: *in situ* compression in a transmission electron microscope and simulations," *Nanotechnology*, vol. 29, no. 8, p. 085703, 2018.
- [31] H. Bhowmick, S. K. Majumdar, and S. K. Biswas, "Influence of physical structure and chemistry of diesel soot suspended in hexadecane on lubrication of steel-on-steel contact," *Wear*, vol. 300, no. 1–2, pp. 180–188, 2013.
- [32] ASTM D 4636-17, "Standard Test Method for Corrosiveness and Oxidation Stability of Hydraulic Oils , Aircraft Turbine Engine Lubricants , and Other Highly," vol. 99, no. Reapproved, 1999.
- [33] A. Turbine and E. Lubricants, "Standard Test Method for Corrosiveness and Oxidation Stability of Hydraulic Oils , Aircraft Turbine Engine Lubricants , and Other Highly," *Order A J. Theory Ordered Sets Its Appl.*, pp. 1–10, 2004.
- [34] A. Al Sheikh Omar, F. Motamen Salehi, U. Farooq, A. Morina, and A. Neville, "Chemical and physical assessment of engine oils degradation and additive depletion by soot," *Tribol. Int.*, vol. 160, p. 107054, 2021.
- [35] A. Al Sheikh Omar, F. M. Salehi, U. Farooq, A. Neville, and A. Morina, "Effect of Zinc Dialkyl Dithiophosphate Replenishment on Tribological Performance of Heavy-Duty Diesel Engine Oil," *Tribol. Lett.*, vol. 70, no. 1, pp. 1–14, 2022.
- [36] K. Jurkiewicz, M. Pawlyta, and A. Burian, "Structure of Carbon Materials Explored by Local Transmission Electron Microscopy and Global Powder Diffraction Probes," *C*, vol. 4, no. 4, p. 68, 2018.
- [37] K. Vyavhare, S. Bagi, M. Patel, and P. B. Aswath, "Impact of Diesel Engine Oil Additives-Soot Interactions on Physiochemical, Oxidation, and Wear Characteristics of Soot," *Energy and Fuels*, vol. 33, no. 5, pp. 4515–4530, 2019.
- [38] P. Toth, D. Jacobsson, M. Ek, and H. Wiinikka, "Real-time, in situ, atomic scale observation of soot oxidation," *Carbon N. Y.*, vol. 145, pp. 149–160, 2019.
- [39] S. Zhang *et al.*, "Control of graphitization degree and defects of carbon blacks through ball-milling," *RSC Adv.*, vol. 4, no. 1, pp. 505–509, 2014.
- [40] B. Gupta, N. Kumar, K. Panda, V. Kanan, S. Joshi, and I. Visoly-Fisher, "Role of oxygen functional groups in reduced graphene oxide for lubrication," *Sci. Rep.*, vol. 7, pp. 1–14, 2017.
- [41] A. D. Sediako, C. Soong, J. Y. Howe, M. R. Kholghy, and M. J. Thomson, "Real-time observation of soot aggregate oxidation in an Environmental Transmission Electron Microscope," *Proc. Combust. Inst.*, vol. 36, no. 1, pp. 841–851, 2017.

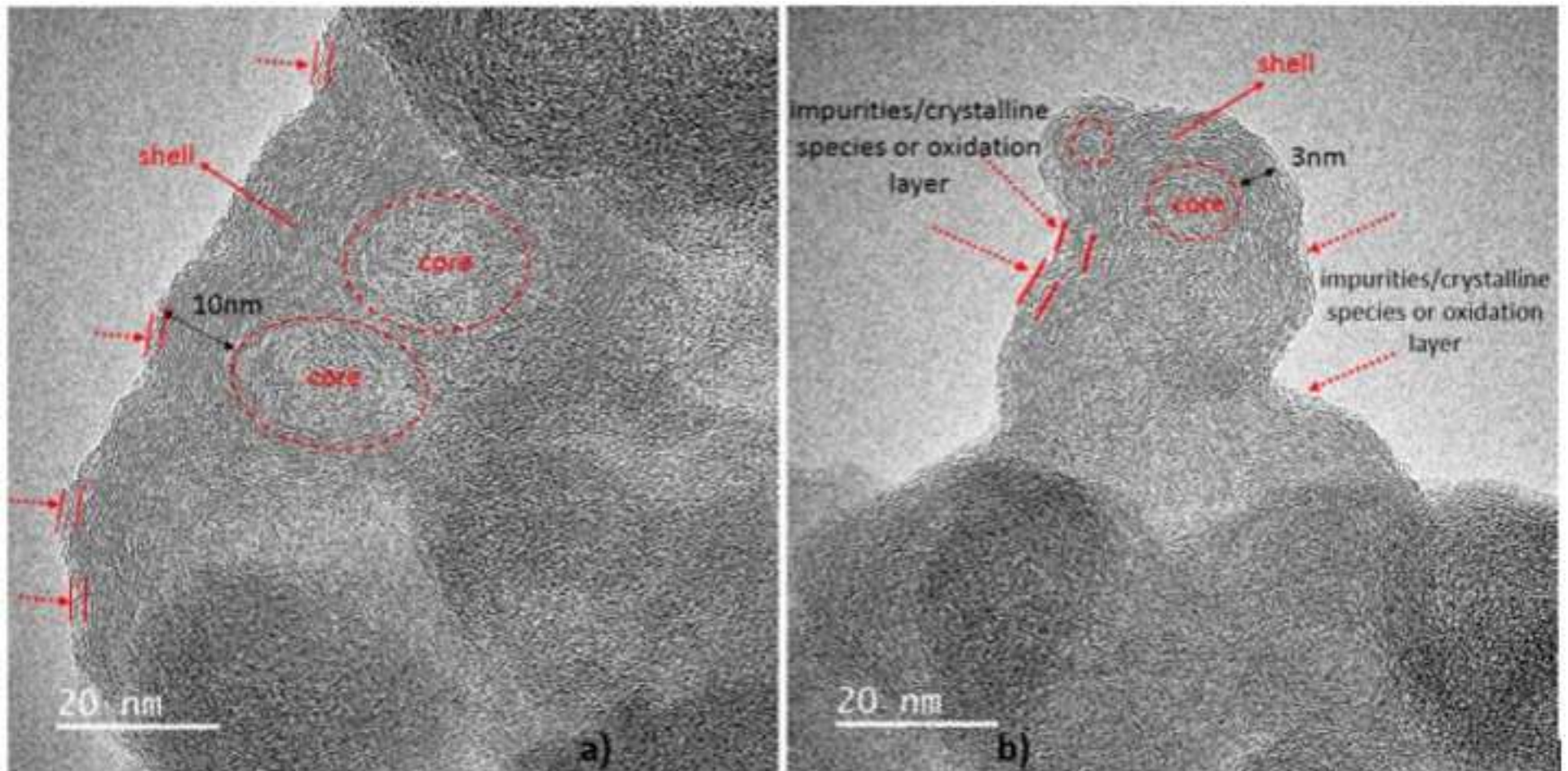
- [42] V. Sharma *et al.*, "Structure and chemistry of crankcase and exhaust soot extracted from diesel engines," *Carbon N. Y.*, vol. 103, pp. 327–338, 2016.

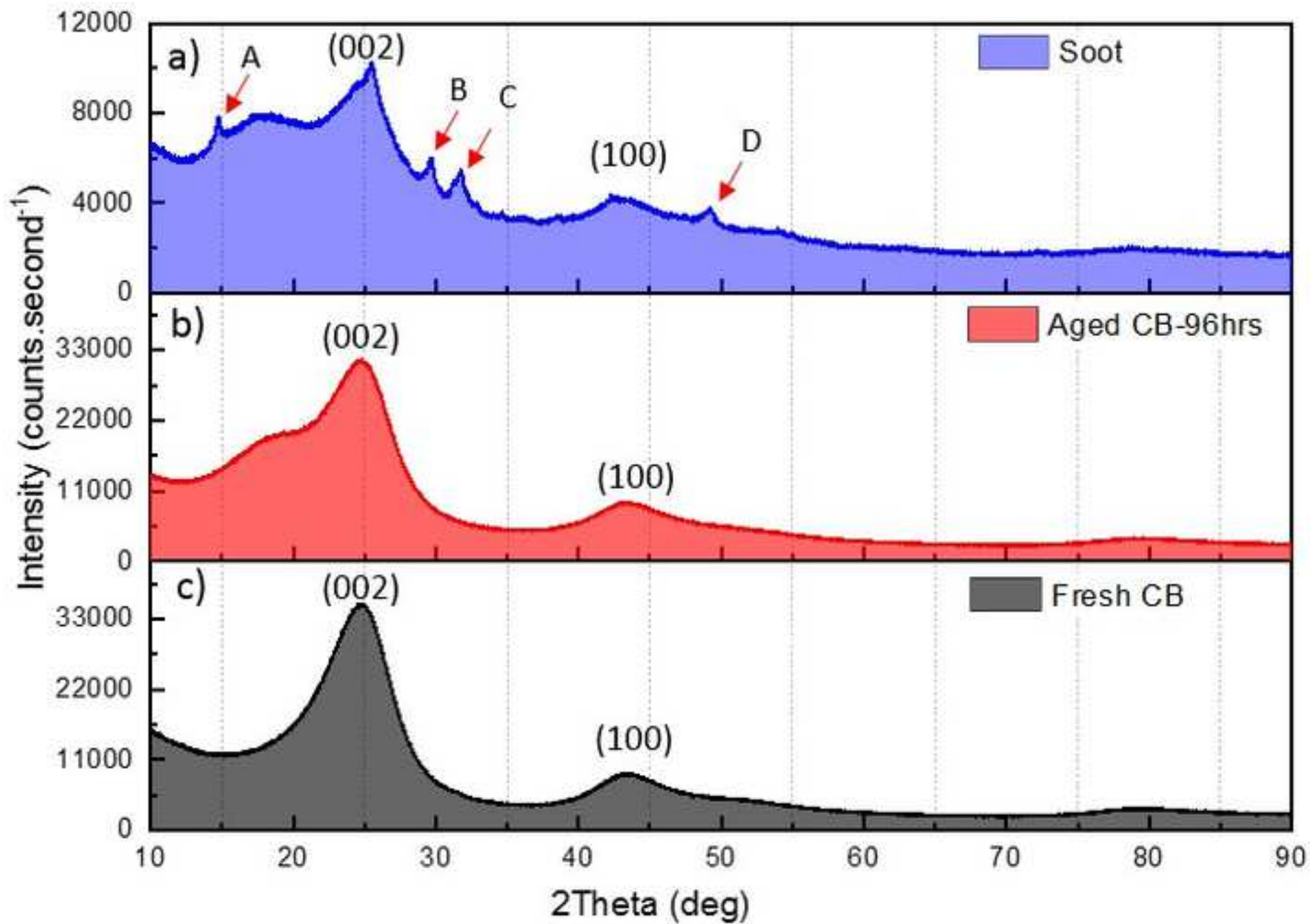


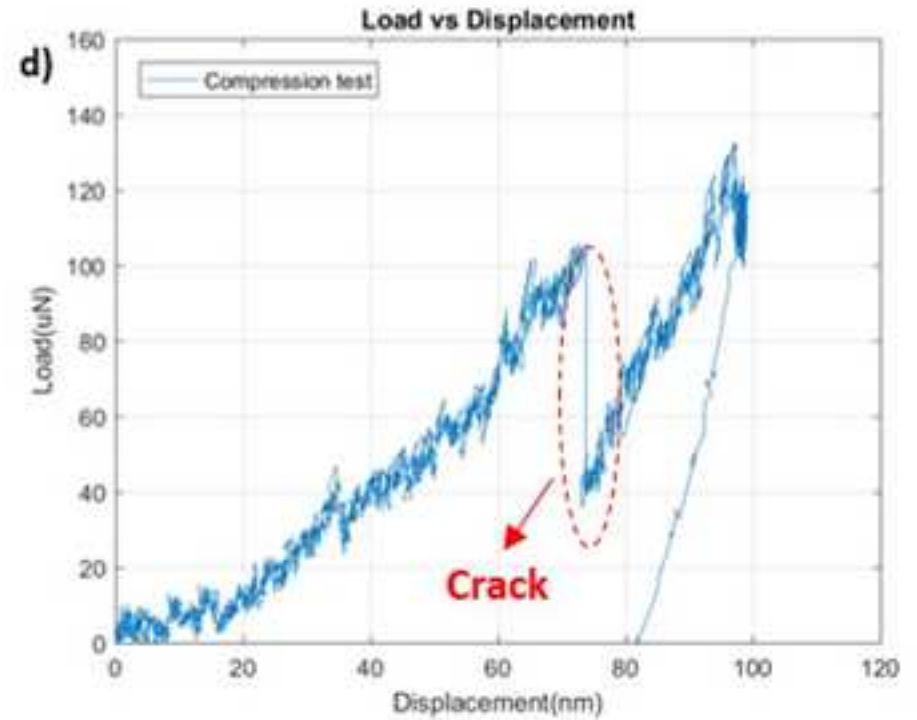
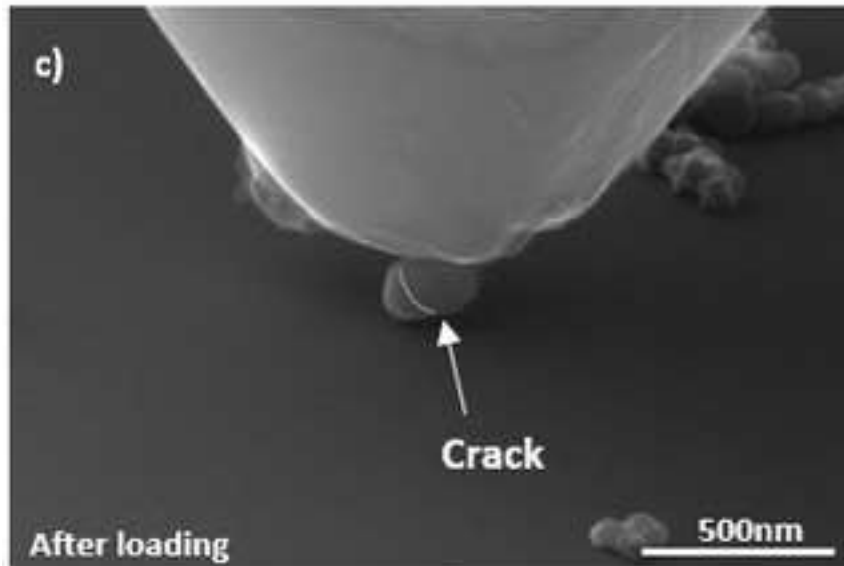
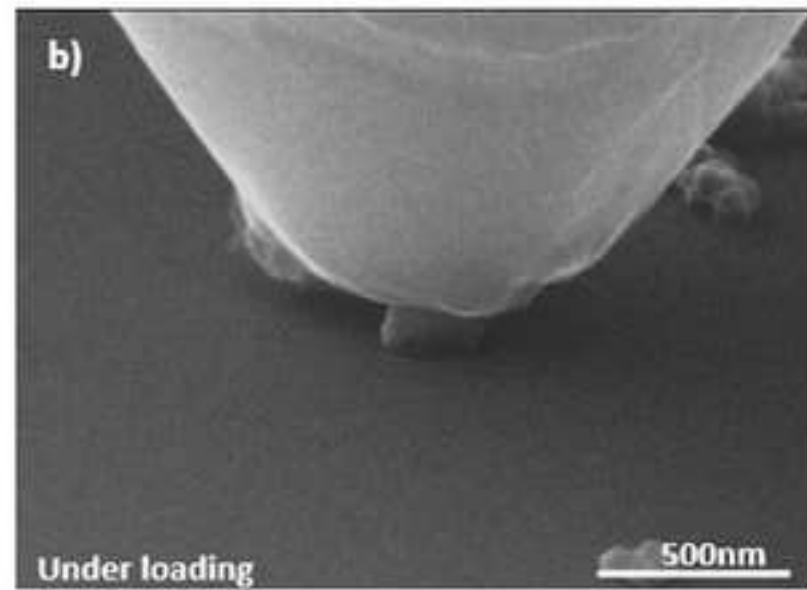
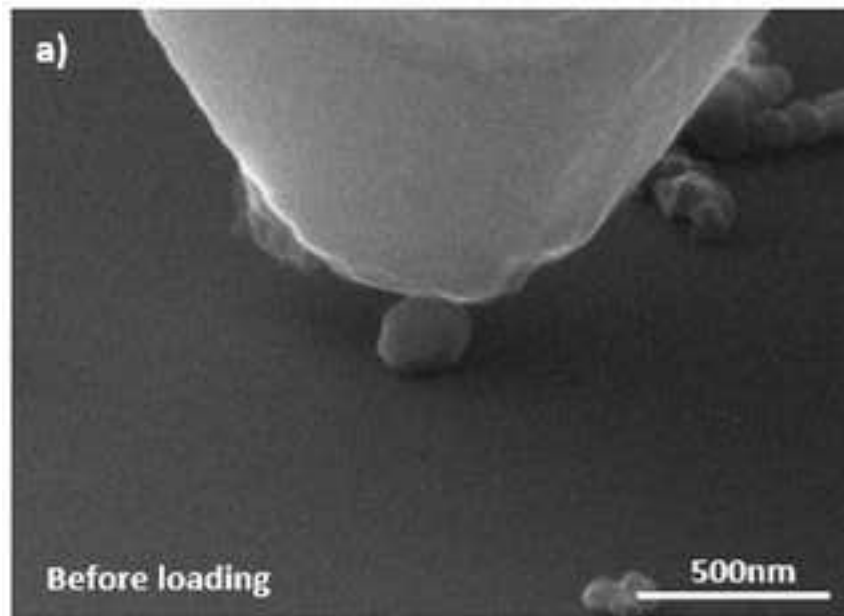


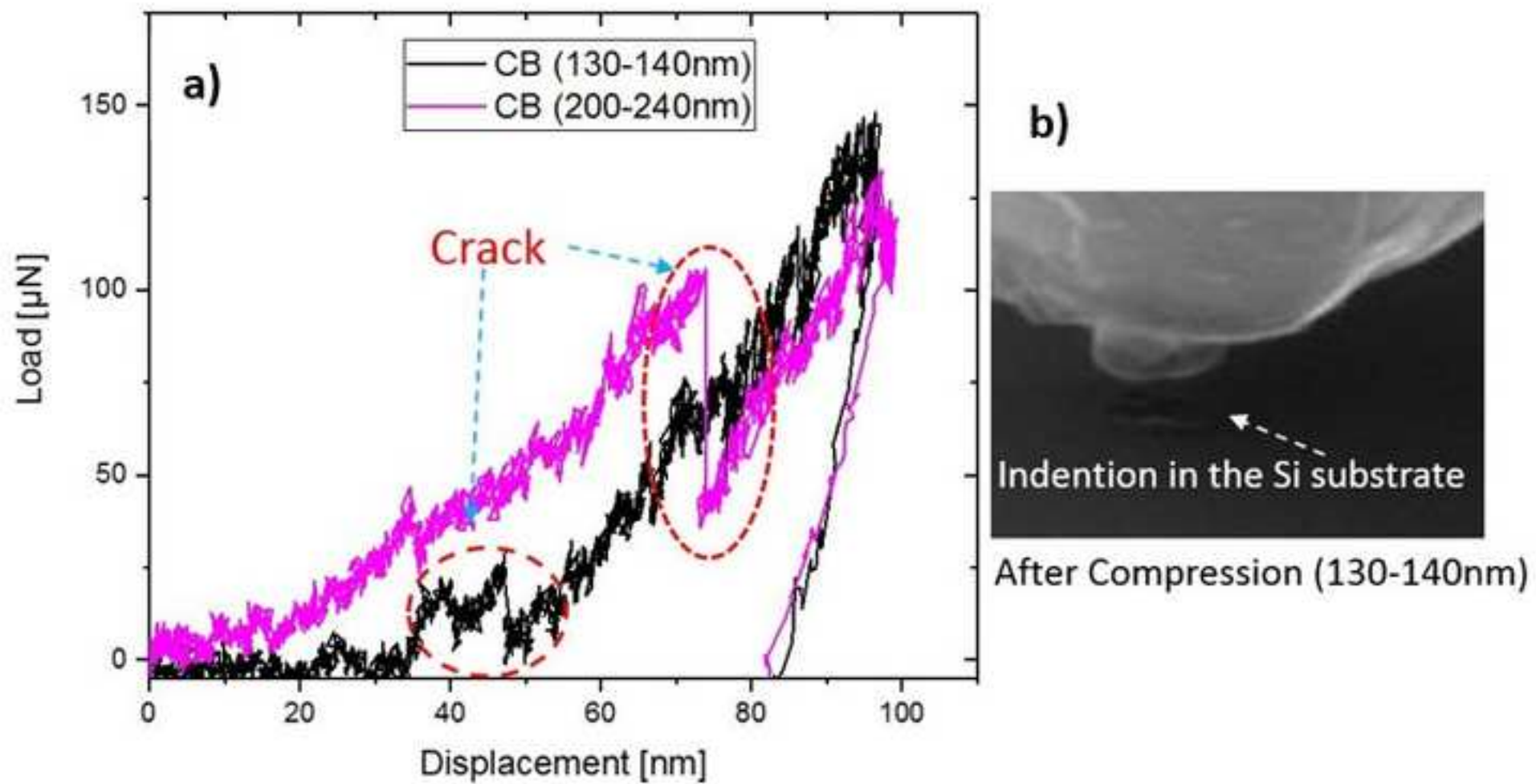


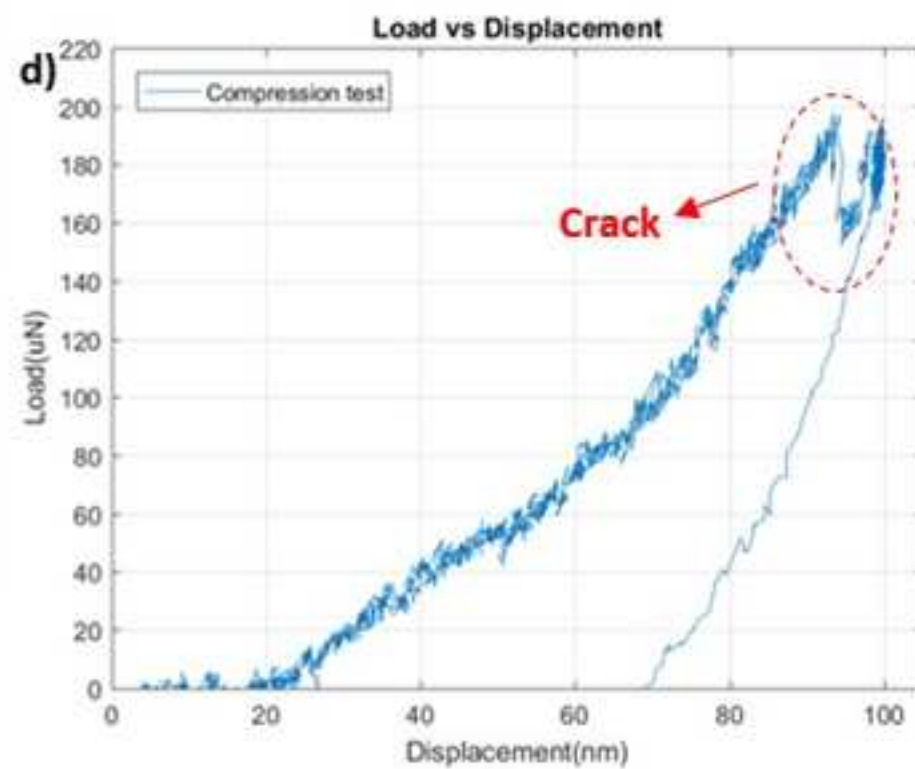
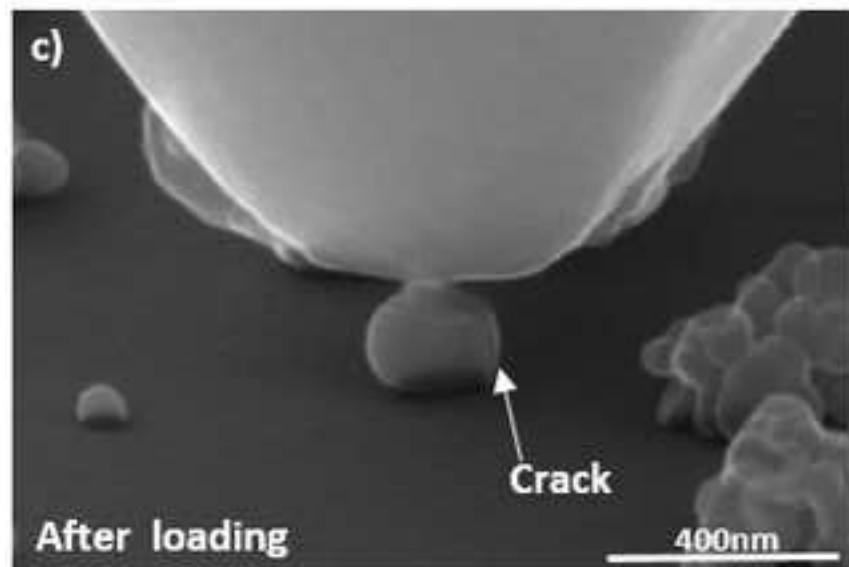
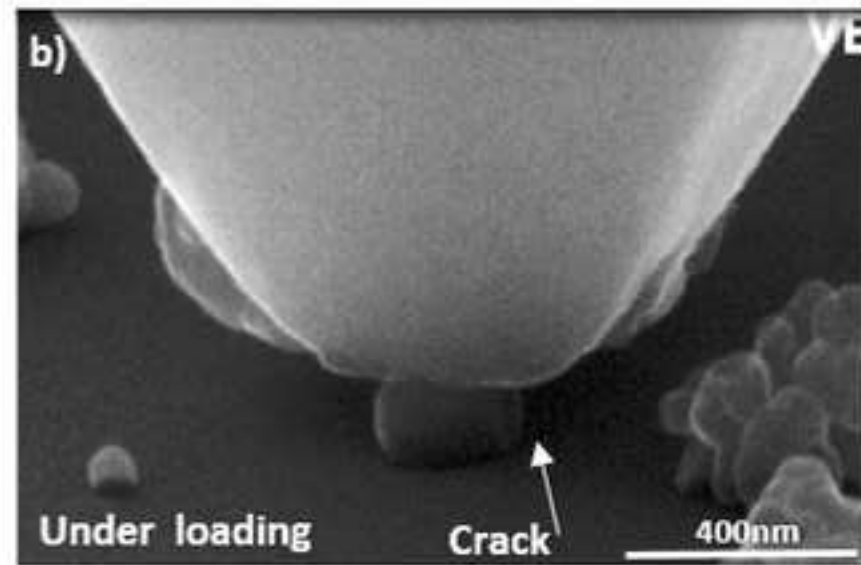
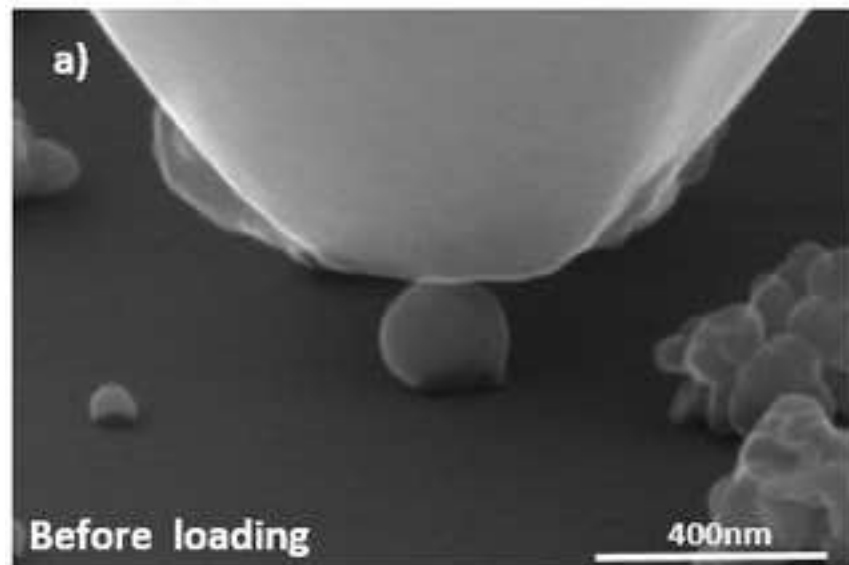


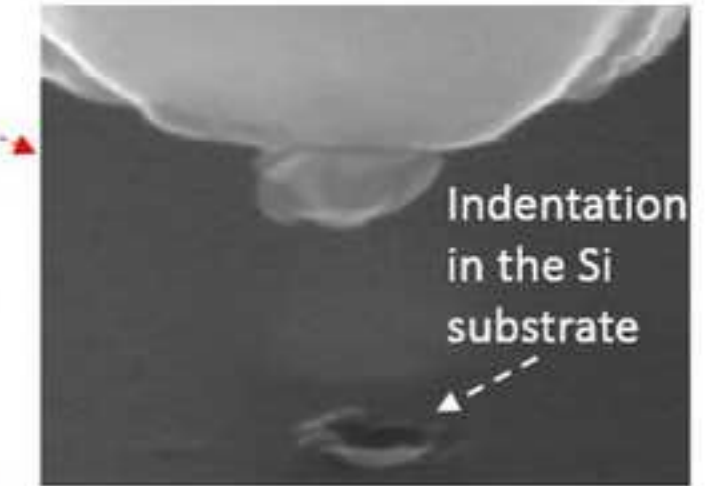
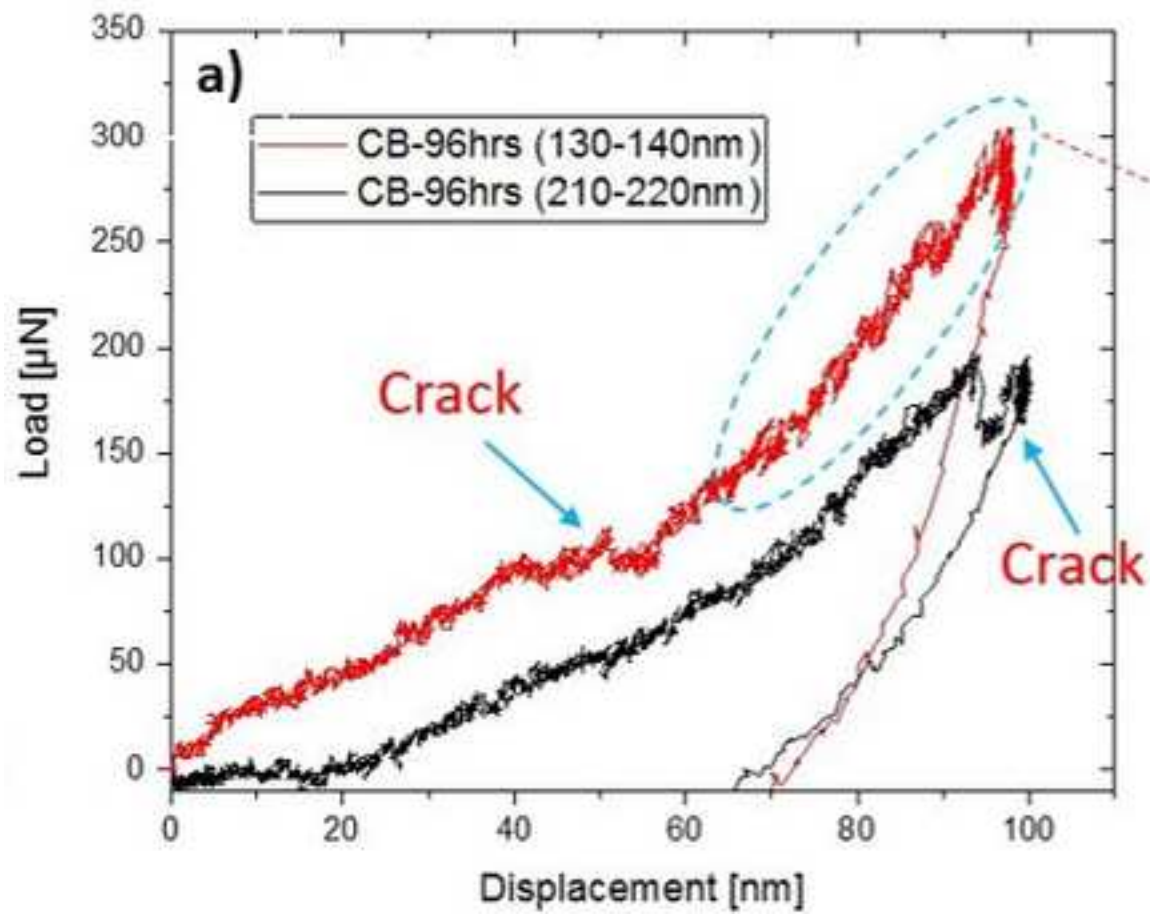












b) After Compression (130-140nm)

